AD NUMBER

AD809420

LIMITATION CHANGES

TO:

Approved for public release; distribution is unlimited.

FROM:

**Distribution authorized to U.S. Gov't. agencies and their contractors;
Administrative/Operational Use; FEB 1967. Other requests shall be referred to Defense Advanced Research Projects Agency, Arlington, VA 22203.**

AUTHORITY

USAEC ltr 30 Jul 1971

TECHNICAL REPORT ECOM-01758-4

GUNN EFFECT DEVICES

FOURTH QUARTERLY TECHNICAL REPORT

By

M.L. WRIGHT

FEBRUARY 1967

ECOM

UNITED STATES ARMY ELECTRONICS COMMAND • FORT MONMOUTH, N.J.

CONTRACT DA 28-043 AMC-01758(E) - ARPA Order No. 692
HEWLETT-PACKARD COMPANY
HEWLETT-PACKARD LABORATORIES
Palo Alto, California

The work prepared under this contract is a part of PROJECT DEFENDER and was made possible by the support of the Advanced Research Projects Agency under Order No. 692, through the U. S. Army Electronics Command.

DISTRIBUTION STATEMENT

DISCLAIMER

The findings in this report are not to be construed as an official Department of the Army position unless so designated by other authorized document.

Destroy this report when no longer needed. Do not return it to the originator.

Technical Report ECOM-01758-4 FEBRUARY 1967

GUNN EFFECT DEVICES

FOURTH QUARTERLY TECHNICAL REPORT
15 August 1966 to 15 November 1966

Report No. 4

Contract No. DA 28-043 AMC-01758(E)
ARPA Order No. 692
O/S Task No. 7900.21.243.38.00

Prepared by

M. L. Wright

HEWLETT-PACKARD COMPANY
Hewlett-Packard Laboratories
Palo Alto, California

for

U. S. Army Electronics Command, Fort Monmouth, New Jersey

The work prepared under this contract is part of PROJECT DEFENDER and was made possible by the support of the Advanced Research Projects Agency under Order No. 692, through the U. S. Army Electronics Command.

ABSTRACT

A third series of devices (PUAS) using commercially available boat-grown material has been fabricated and tested. This series is slightly thinner than the previous runs and shows a slightly lower threshold and a slightly higher Gunn frequency; in all respects they are quite similar to the previous results. The estimated contact resistance for the PUAS devices is about 8% of the bulk resistance.

Gunn effect devices have also been made from solution-grown GaAs material produced by Hewlett-Packard Laboratories. These devices show a positive temperature coefficient and thus require less power to operate. The noise level produced by these devices is lower than for the devices using boat-grown material especially at higher frequencies (~100Kc).

A circuit simulation for the Gunn device has been programmed for computer device-circuit interaction studies. This circuit model retains both the nonlinear and time-dependent characteristics of the device and has shown good correlation with several experimental results.

PURPOSE

A development program is to be conducted aimed at the utilization of the Gunn effect for various types of microwave generating devices in the 1 to 50 GHz frequency range. Spectral line width should be less than 10kHz and operation should be in a single mode. Output power should be at least 25 mW in CW operation and 3W peak in pulsed operation with a conversion efficiency of at least 3%. CW operation should be obtained in ambient temperatures from -25°C to +50°C with a single device.

Application of these devices for amplification and modulation is to be investigated.

FOREWORD

The work reported on in this report has been authorized by the Contracting Officer, Mr. Edgar D. Fitzgerald, Electronic Components Laboratory, U. S. Army Electronics Command, Ft. Monmouth, New Jersey, under Contract No. DA 28-043 AMC-01758(E) and titled "Gunn Effect Devices". The Project Engineer at the U. S. Army Electronics Command is Mr. Maurice Druesne.

The work has been performed at Hewlett-Packard Laboratories under the supervision of M. L. Wright. The report has been prepared by M. L. Wright. Significant contributions during the report period have been made by T. O. Yep, G. W. Mathers, E. Gowen and B. Farrell. Discussions with M. M. Atalla and C. F. Quate were of great benefit.

TABLE OF CONTENTS

GUNN EFFECT DEVICES

FOURTH QUARTERLY TECHNICAL REPORT

I. DEVICE FABRICATION AND MEASUREMENTS

I.1 Introduction

The emphasis of the work during this quarter has been on the measurement of noise characteristics of Gunn device oscillators. Measurements have been made on devices fabricated from both the boat-grown GaAs material used previously and from the solution-grown material produced recently by Hewlett-Packard Laboratories. Some improvement in noise performance has been noted relative to earlier devices.

Two types of noise have been investigated, the first being low frequency noise from about 20 Hz to 1 MHz; and the second being demodulated FM noise associated with the microwave oscillation. This demodulated FM noise is measured in the same frequency range as the low frequency noise but describes the noise performance as a microwave oscillator.

I.2 Operating Electrical Characteristics

a. Recent Boat-Grown Devices (PUAS-1)

A third series of devices (PUAS-1) have been prepared from one ohm-cm boat-grown GaAs material. These devices are the same physically as the ES-8 devices except that they are slightly thinner, and thereby have a lower threshold voltage and a higher Gunn frequency. They do, however, operate at higher currents because of the greater change in resistance with temperature for this particular slice of material. The resistance change with temperature for the two series of devices is shown in Fig. 1. A significant number of these units have been operated CW and have all shown essentially the same behavior, this being very similar to the ES-8 devices. The preferred frequency tuning range is somewhat higher than that of the ES-8 samples (3.0 to 7.5 GHz) as in the Gunn frequency ($\simeq$ 6.5 GHz).

In Figure 2 the voltage-current characteristics are shown for the ES-8, PUAS-1 and TE-34 devices. The larger temperature coefficient of resistance for the PUAS-1 devices is evident from the higher current required for CW operation. The TE-34 curve will be discussed below. The power output vs. frequency for a representative PUAS-1 device is shown in Figure 3.

Thermal Resistance

The thermal resistance of the PUAS devices with the standard asymmetric geometry was obtained in the following manner. Pulsed I-V curves of the PUAS device were taken at various temperatures from 26°C to 76°C in an oven. Another I-V curve with the device in CW operation was measured with the ambient temperature of the device below room temperature.

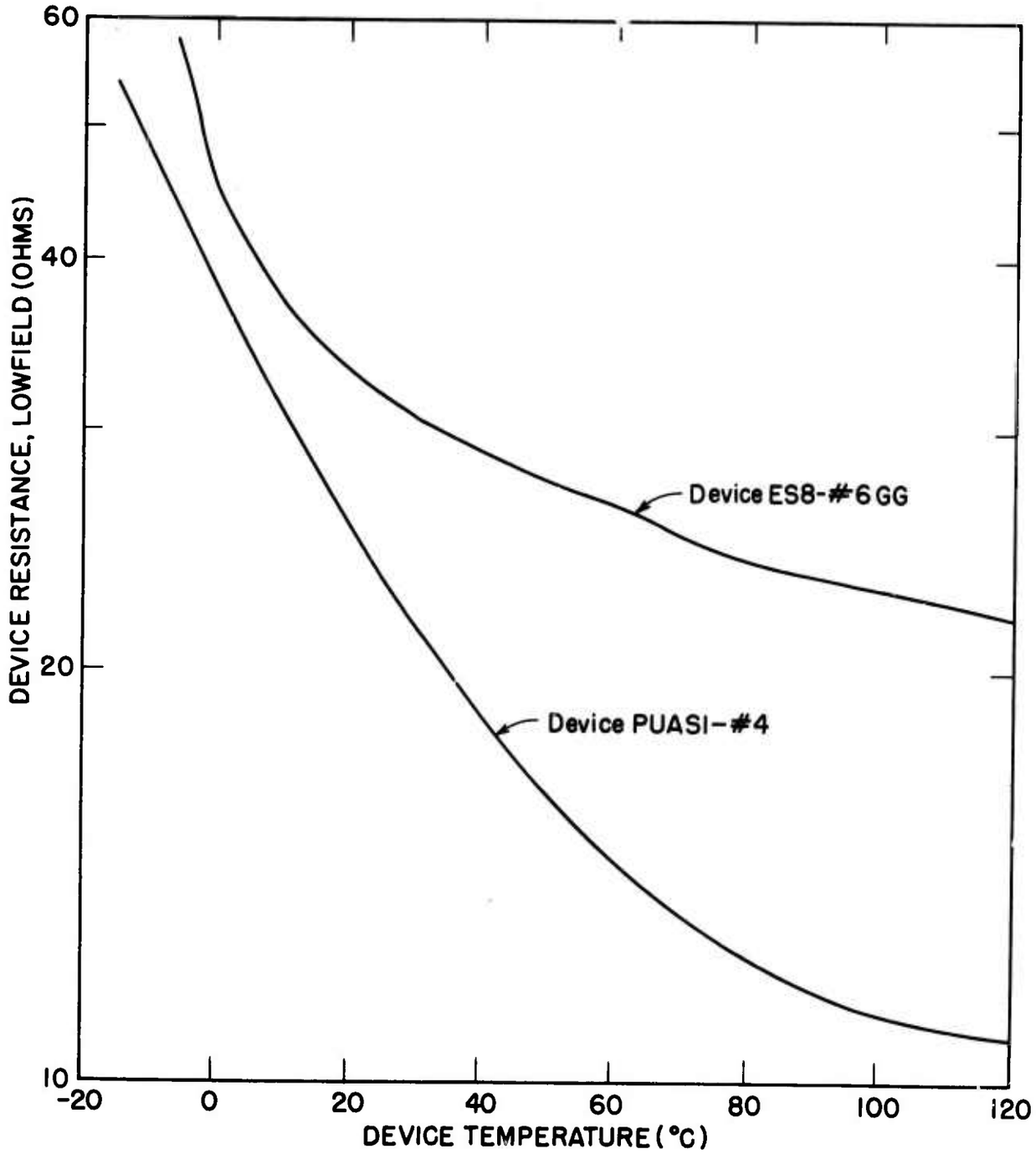

FIGURE 1: Temperature Dependence of Low Field Device Resistance

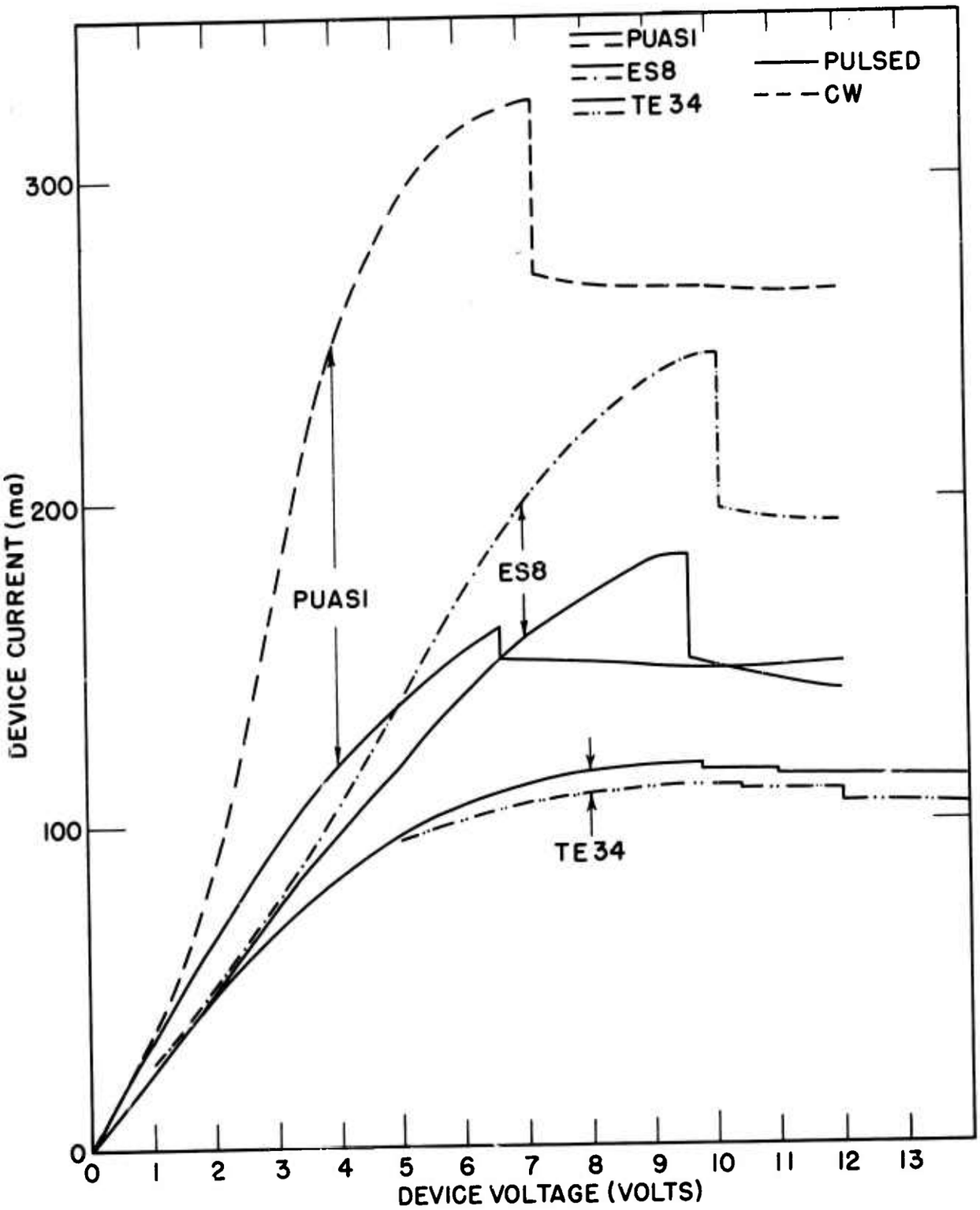

FIGURE 2: Comparison of Recent Device Current-Voltage Characteristics

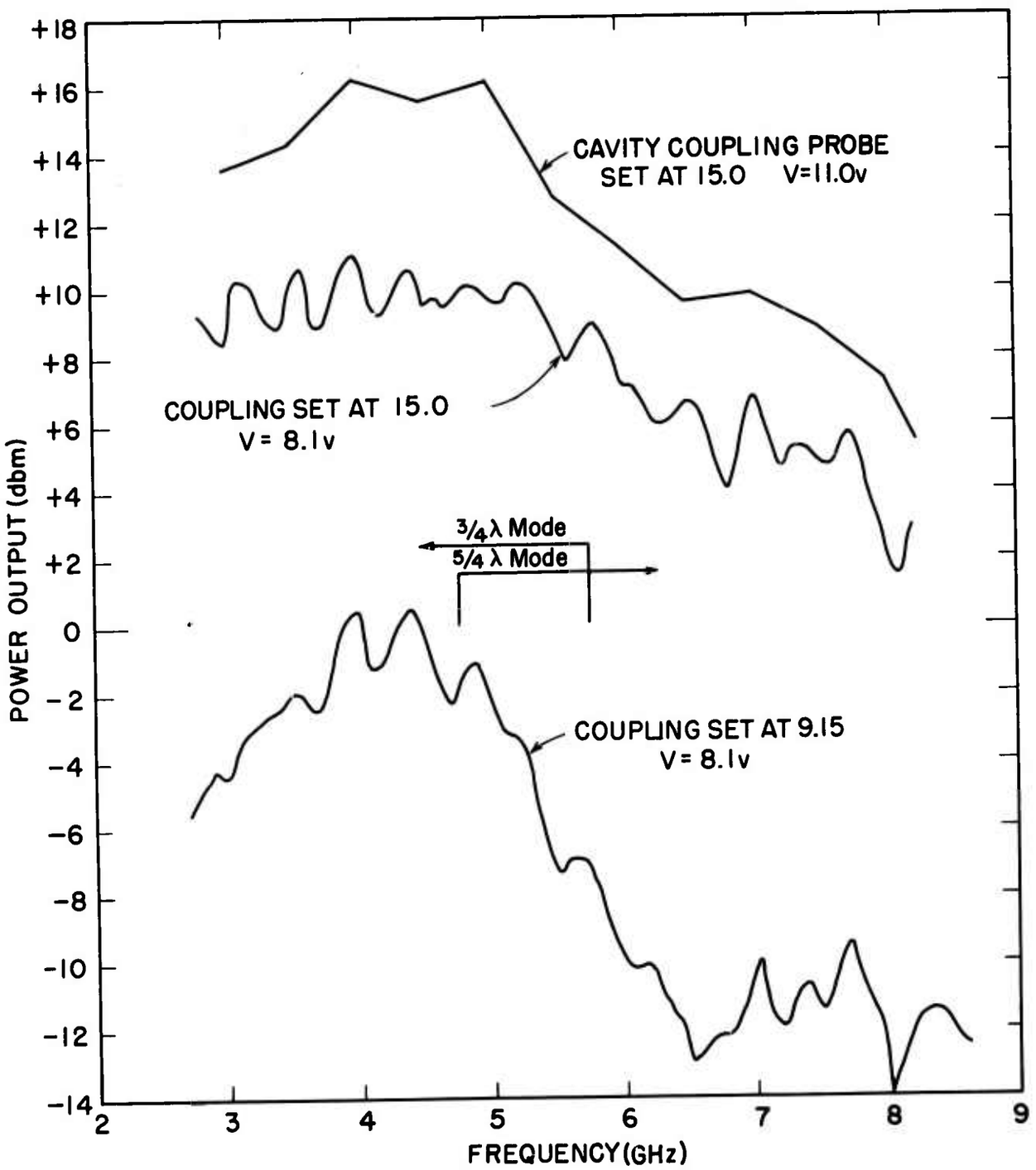

FIGURE 3: Power-Frequency Performance

The intersection of the CW I-V curve with one of the pulsed I-V curves provides the operating temperature of the device at a particular CW power level. The thermal resistance of the device averaged over 26°C to 76° above ambient temperature was found to be 46.6°C/W.

Device Temperature Coefficient

The resistance of the electrically active GaAs material in the Gunn device constitutes the bulk resistance R_B of the device. However, the device resistance, R_D, may or may not consist of a contact resistance, R_C, in addition to the bulk resistance. A comparison between the temperature dependence of the bulk resistance and of the device resistance would reveal the presence of the contact resistance and the temperature range at which it is significant. The device resistance as a function of temperature was obtained by passing a current of 10 mA through the device, which was in an environmental oven, and measuring the voltage across the device. The bulk resistivity, ρ, was measured by standard potentiometric techniques at various temperatures on a Hall plate prepared from a neighboring slice of GaAs material for the PUAS-1's and RE-2's. To find the bulk resistance, the ratio of the thickness, t, to the cross section, A, of the electrically active portion of the GaAs must be determined, since

$$R_B = \rho \times \frac{t}{A} \quad . \tag{1}$$

The ratio of the device resistance to the bulk resistivity at any temperature can be expressed as

$$\frac{R_D}{\rho} = \frac{t}{A} \left(1 + \frac{R_C}{R_B} \right) , \tag{2}$$

which would reduce to

$$\frac{R_D}{\rho} \sim \frac{t}{A} \qquad (3)$$

for $R_C/R_B << 1$. Figure 4 contains plots of R_D/ρ versus the temperature for two PUAS-1 devices, viz. #4 and #9. From the two curves, R_D/ρ varies with temperature below 55°C, but at sufficiently high temperatures R_D/ρ is a constant with temperature. The significance of the saturated R_D/ρ values at the higher temperatures is that at these temperatures $R_C/R_B << 1$ from considerations of approximate measurement of t and A and thus, $R_D/\rho \sim t/A$. The geometric factors, t/A, for PUAS-1 #4 and for PUAS-1 #9 are 13.5 cm^{-1} and 15.6 cm^{-1}, respectively. Plots for PUAS-1 #4 of the bulk resistance calculated from Eq. (1) using the above determined t/A value, 13.5 cm^{-1}, and of the device resistance as a function of temperature are shown in Figure 5. Similar curves for PUAS-1 #9 are presented in Fig. 6. Figures 5 and 6 indicate that the device resistance and bulk resistance are not equal at the lower temperatures. However, the R_D and R_B curves do converge towards one another with increasing temperature and coincide for temperatures above ~60°C. The difference between device resistance and the bulk resistance is the contact resistance. At room temperature the contact resistance is ~8% of the device resistance.

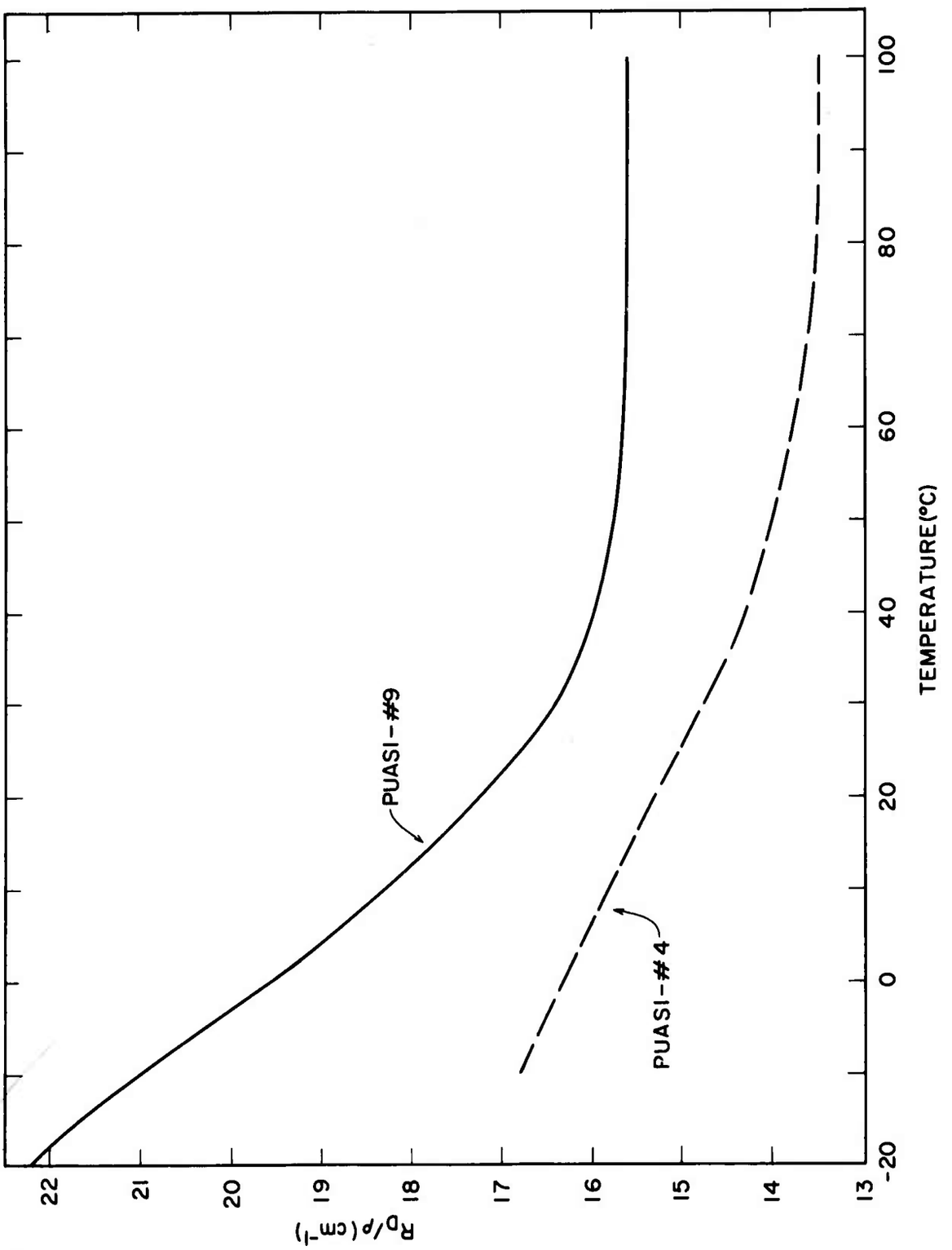

FIGURE 4: Normalized resistance-Temperature Characteristics

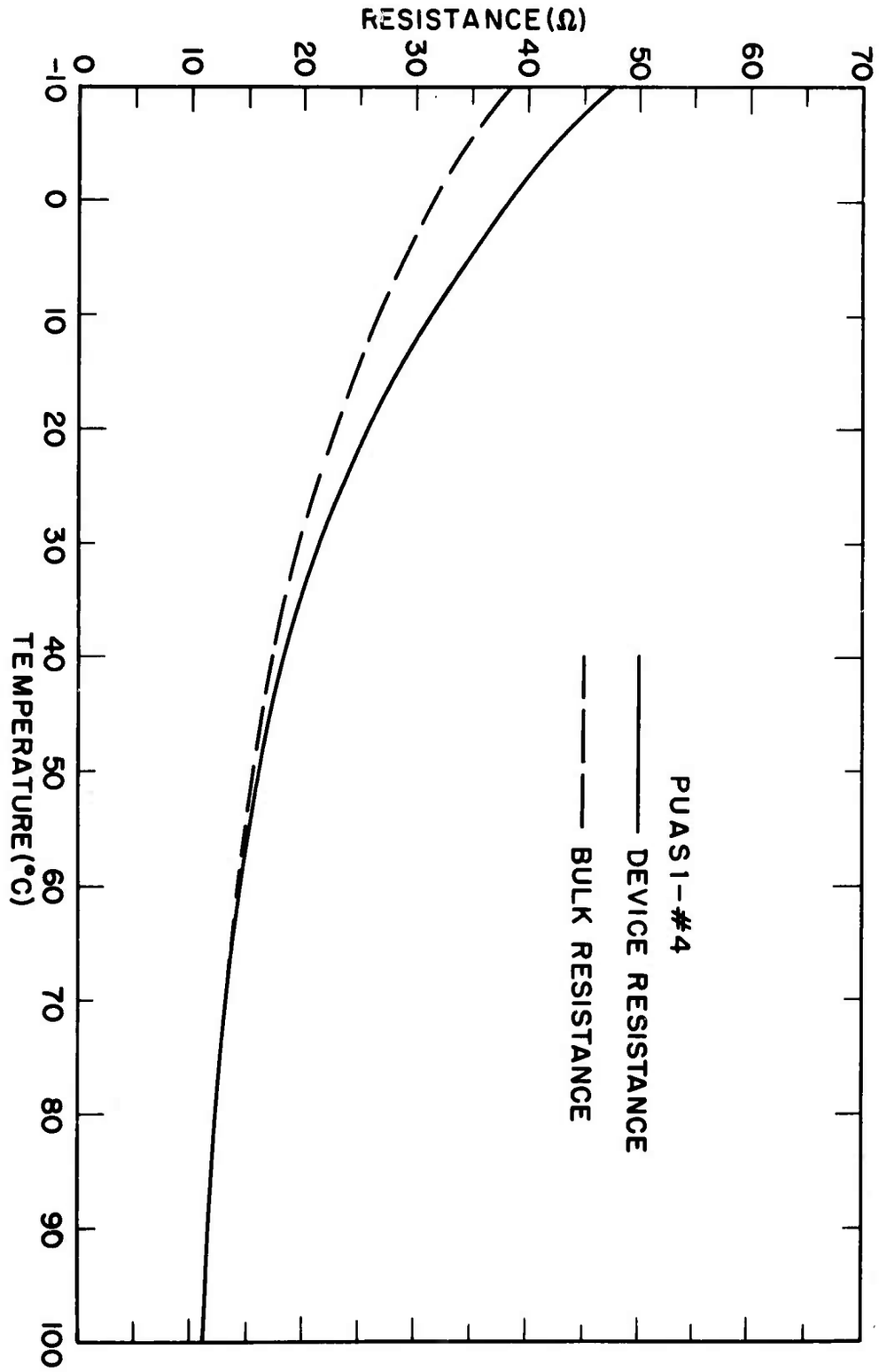

FIGURE 5: Resistance-Temperature Characteristics

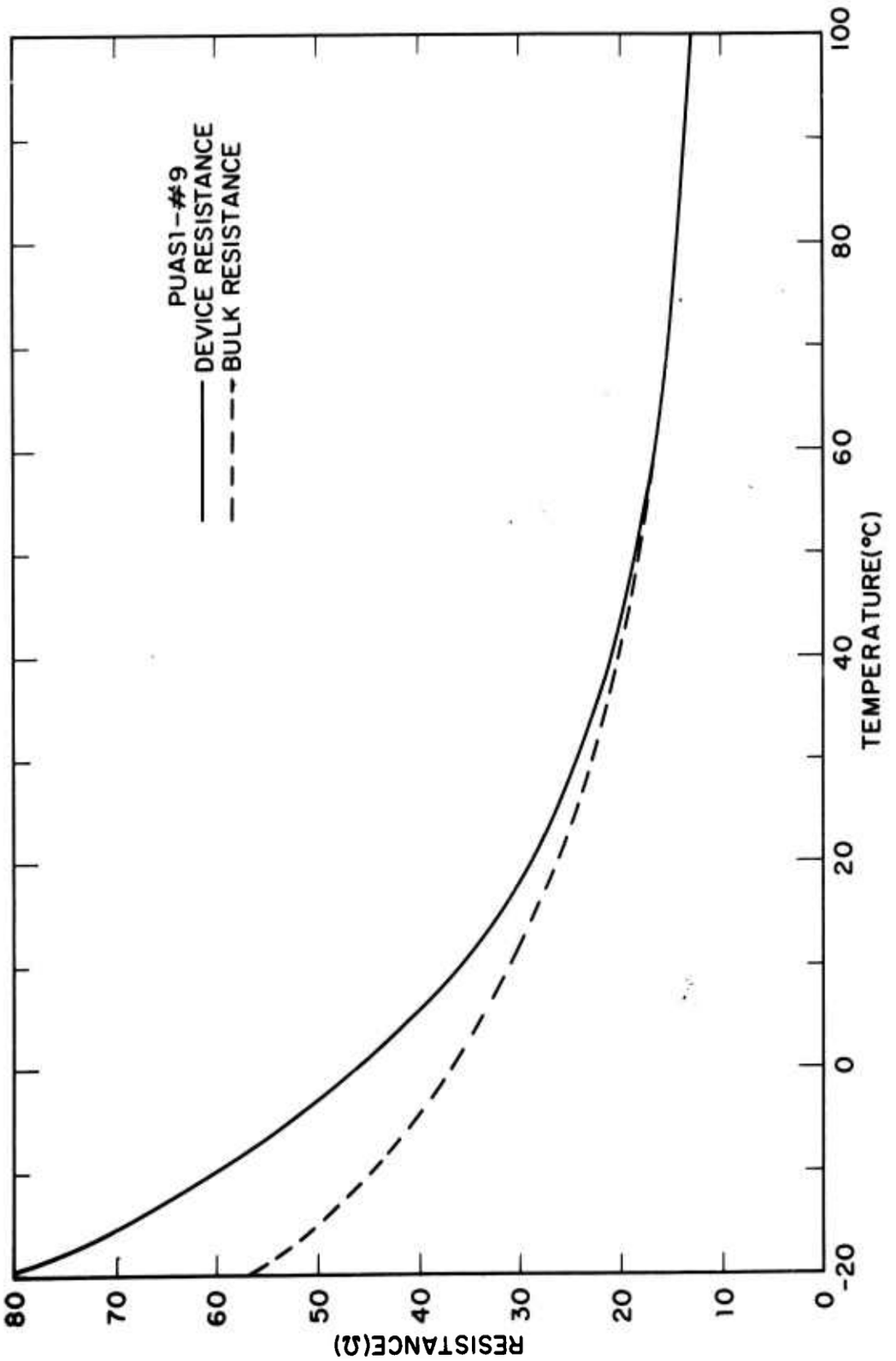

FIGURE 6: Resistance-Temperature Characteristics

b. Solution Grown Epitaxial Devices

A fourth series of devices (TE-34) made with Hewlett-Packard Laboratories solution grown epitaxial material have been constructed and mounted. As yet the number of these devices tested has not been sufficient to establish a definite behavior norm, but the samples do show a positive resistance vs. temperature coefficient as is shown in Fig. 2. As a result the TE-34 devices operate CW at lower current and dc power levels than the ES-8 or PUAS-1 devices.

I.3 Noise Measurements

The emphasis this last quarter has been on evaluating the noise performance of these devices when operated in a coaxial resonant cavity using the ES-8 devices, PUAS-1 devices and more recently the TE-34 devices.

The r.m.s. frequency deviation in a 1 KHz bandwidth at a modulation frequency of 10 kHz has been measured for several devices of each type versus cavity tuning, applied dc voltage and cavity Q. Typical results are illustrated in Figs. 7 and 8. Also the r.m.s. frequency deviation at a modulation frequency of from 30 c/s to 1 mc/s has been measured for several devices under different operating conditions (dc voltage, tuning, cavity Q, etc.). All of the ES-8 and PUAS-1 devices tested have shown essentially the same behavior with about 2:1 spread in magnitude of r.m.s. frequency deviation at a given modulation frequency. However, two TE-34 devices tested so far have shown quite a different behavior with a significant decrease in the F.M. noise at higher (100 KHz to 1 MHz) modulating frequencies. This is well illustrated in Fig. 9 and in the spectrum photograph (Fig. 10).

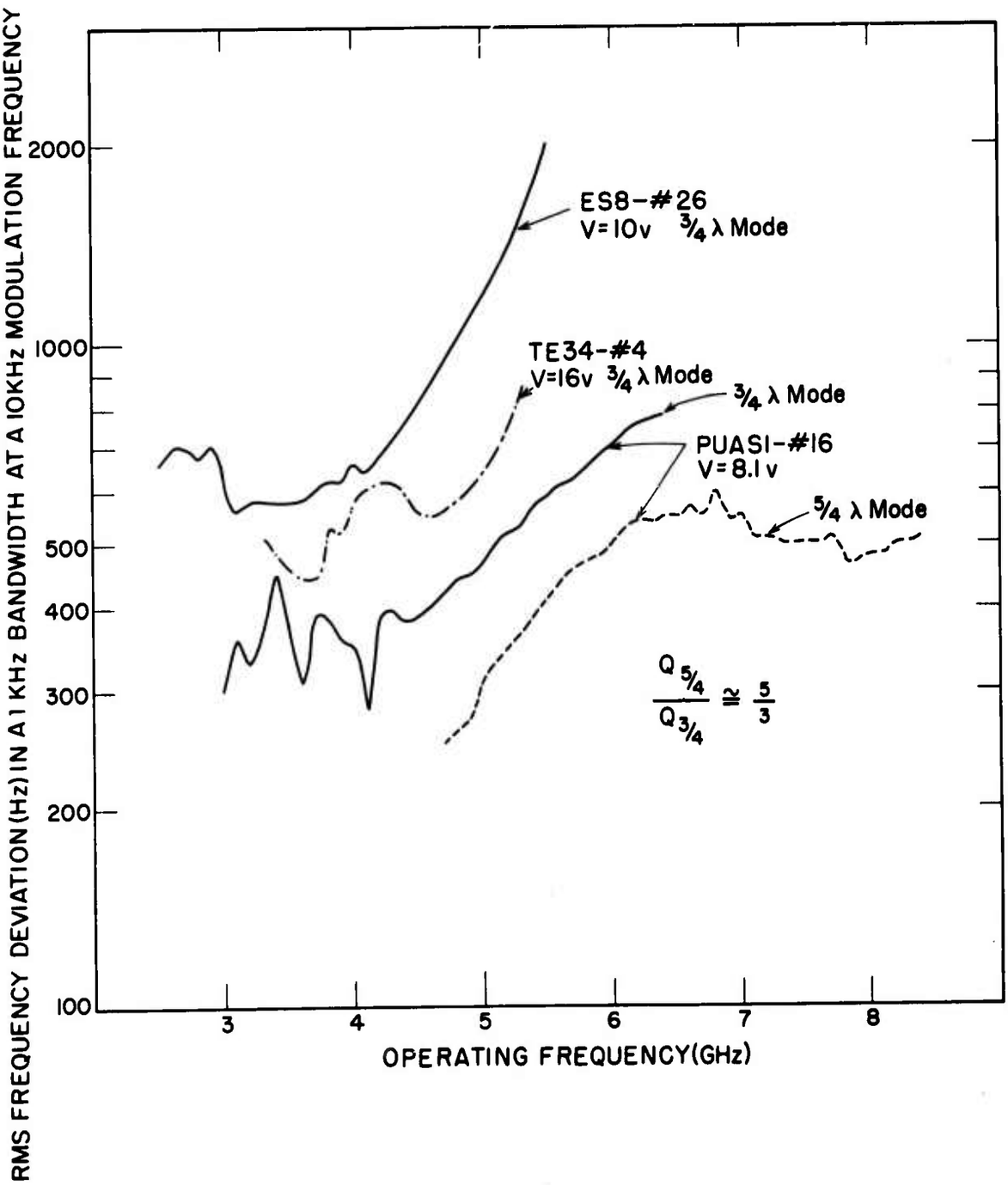

FIGURE 7: FM Noise Performance vs. Operating Frequency

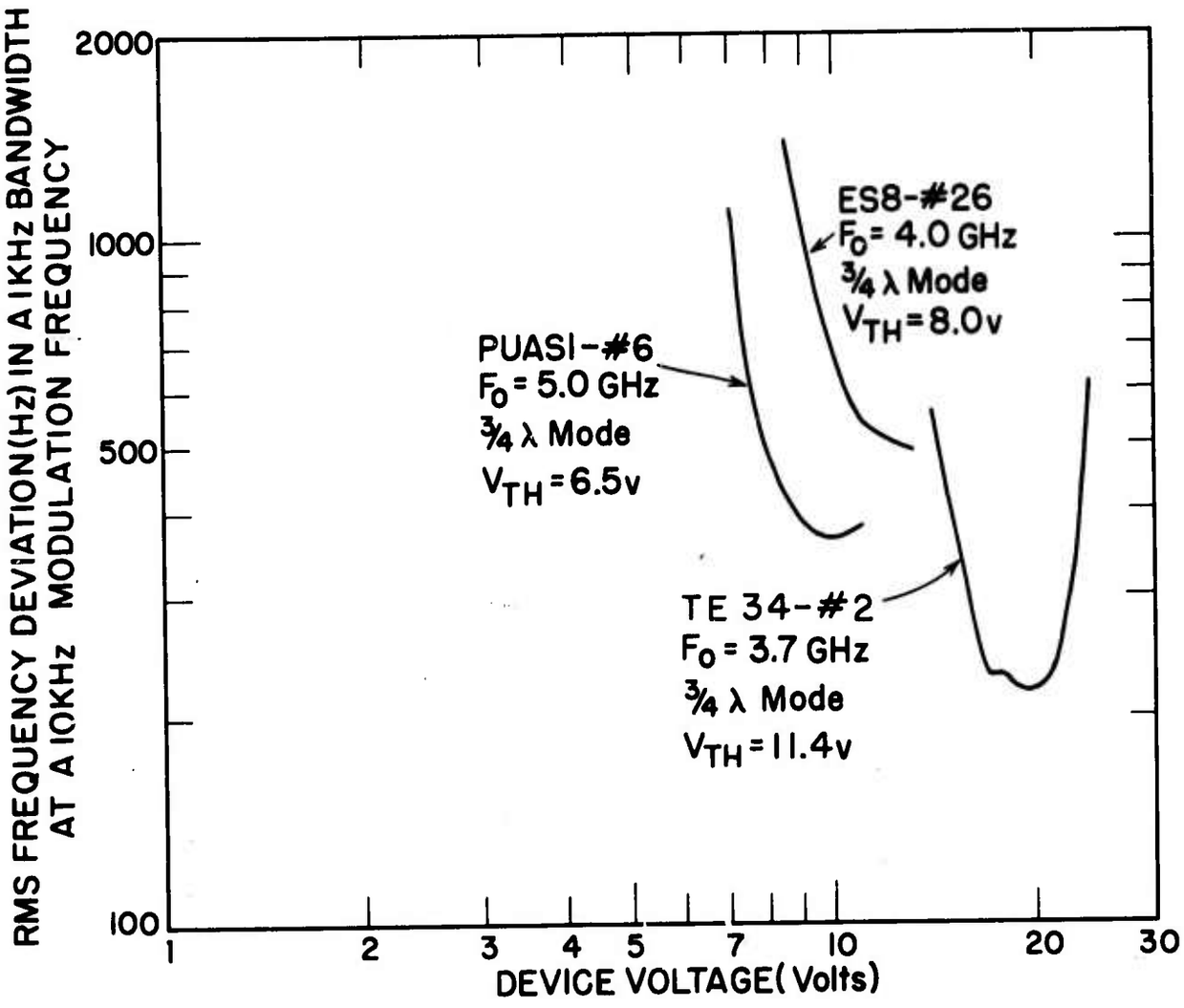

FIGURE 8: FM Noise Performance vs. Bias Voltage

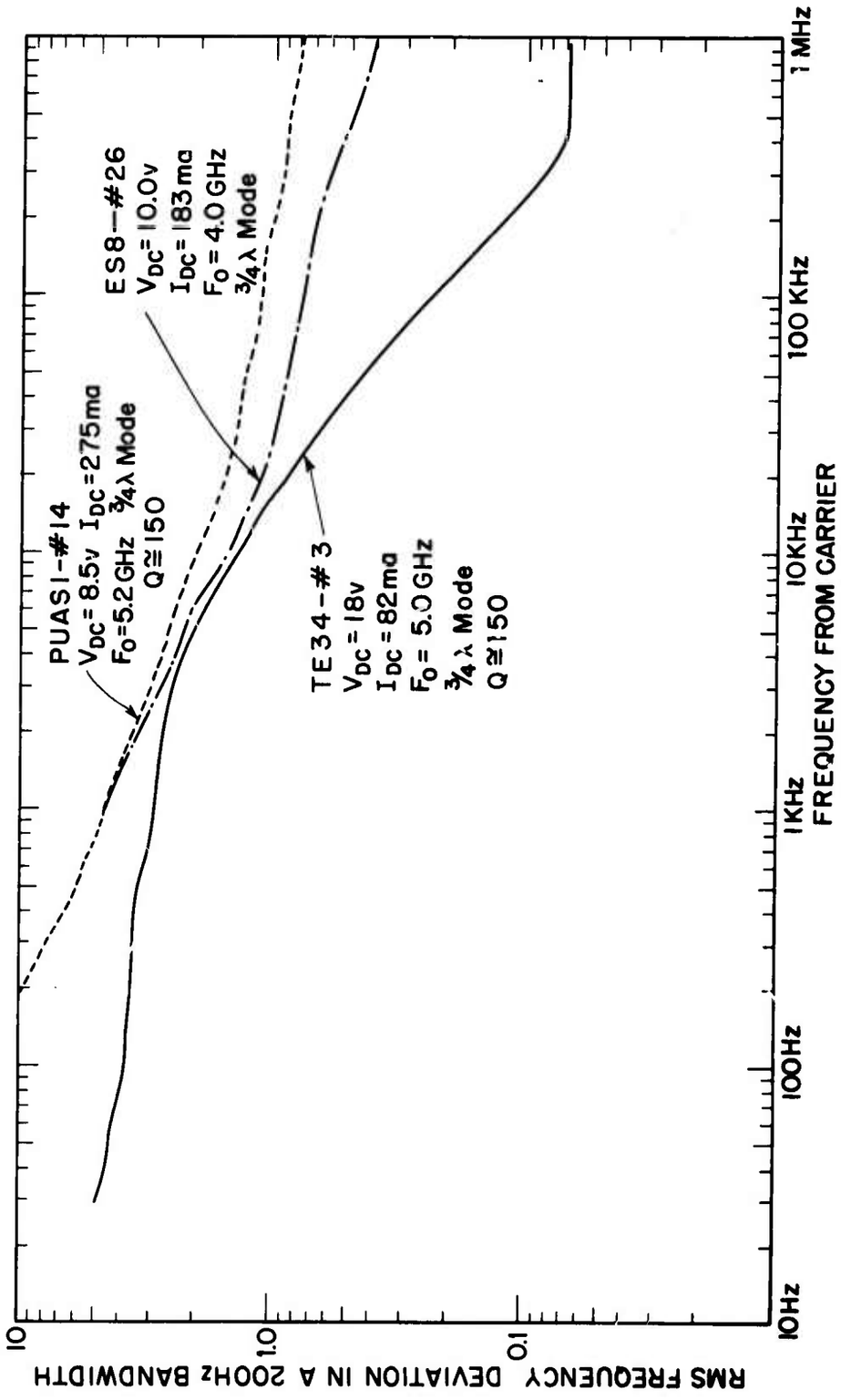

FIGURE 9: Frequency Spectrum of Demodulated FM Noise

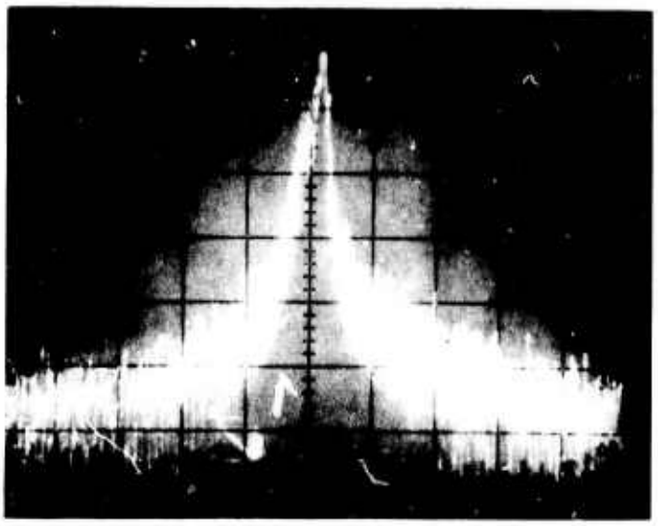

A. PUAS-1

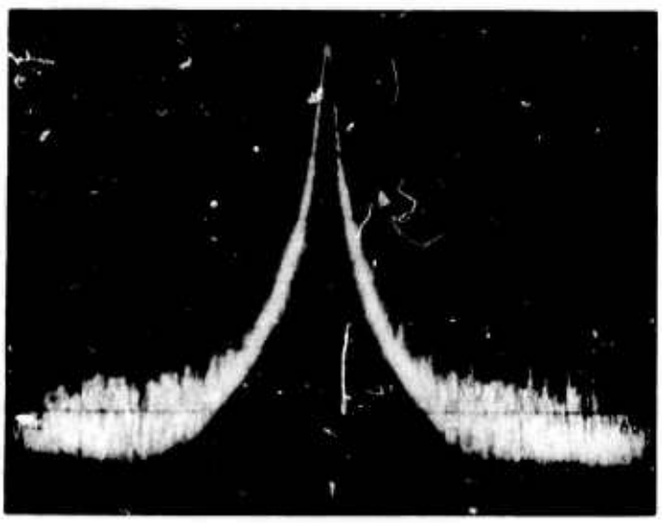

B. TE-34

FIGURE 10: Measured Noise Spectra of Recent Devices

In addition to the demodulated R.F. noise, extensive tests have been made of the video noise produced by the devices when operated both below and above threshold. As shown in Fig. 11, for the ES-8 and PUAS-1 devices the shortcircuit video noise current below threshold increases linearly with device current then tends to saturate as the device current saturates. For the TE-34 devices the short circuit video noise current increases linearly with device current at first, then seems to increase as some power of the dc current. This latter behavior is somewhat different for the two devices so far tested.

Although no direct correlations have been attempted in relating the video noise to the r.f. noise, they both appear to have these similar characteristics and behavior:

1. The video noise above threshold and slightly below threshold has the same frequency behavior in the 1 KC to 1 MC range as the demodulated r.f. noise (Compare Fig. 9 and Fig. 12).
2. The video noise above threshold varies at about the same rate with device voltage as the demodulated r.f. noise.
3. On several devices that have changed characteristics due to operation at high dc power inputs the video noise above and just below threshold as well as the r.f. noise have both increased although not necessarily by the same amount.

I.4 Additional Device Investigations

To reduce the effect of the high field present near the edge of the circular dot in the present asymmetric contact configuration, a hole configuration

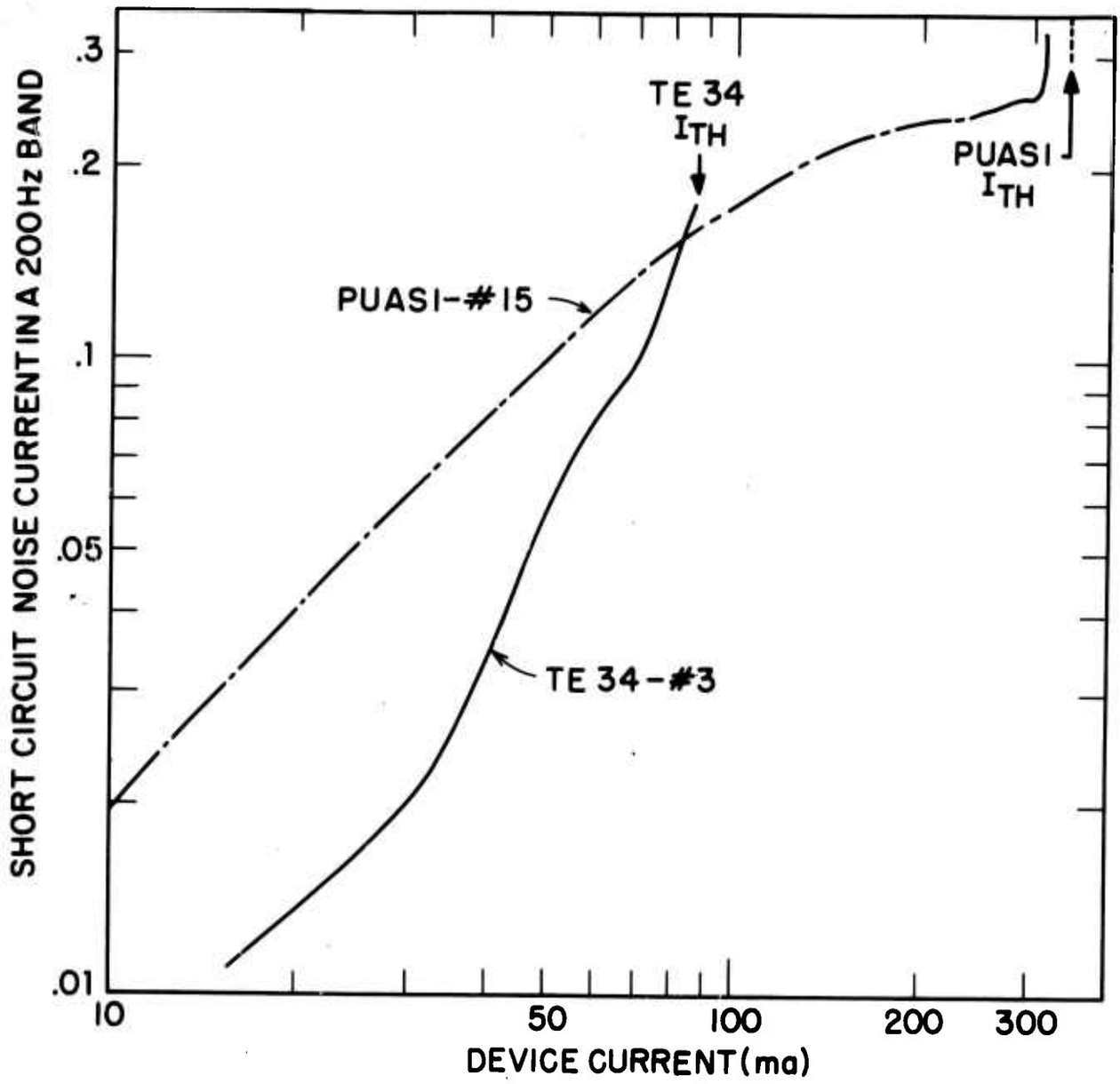

FIGURE 11: Low Frequency Noise Current vs. Device Current

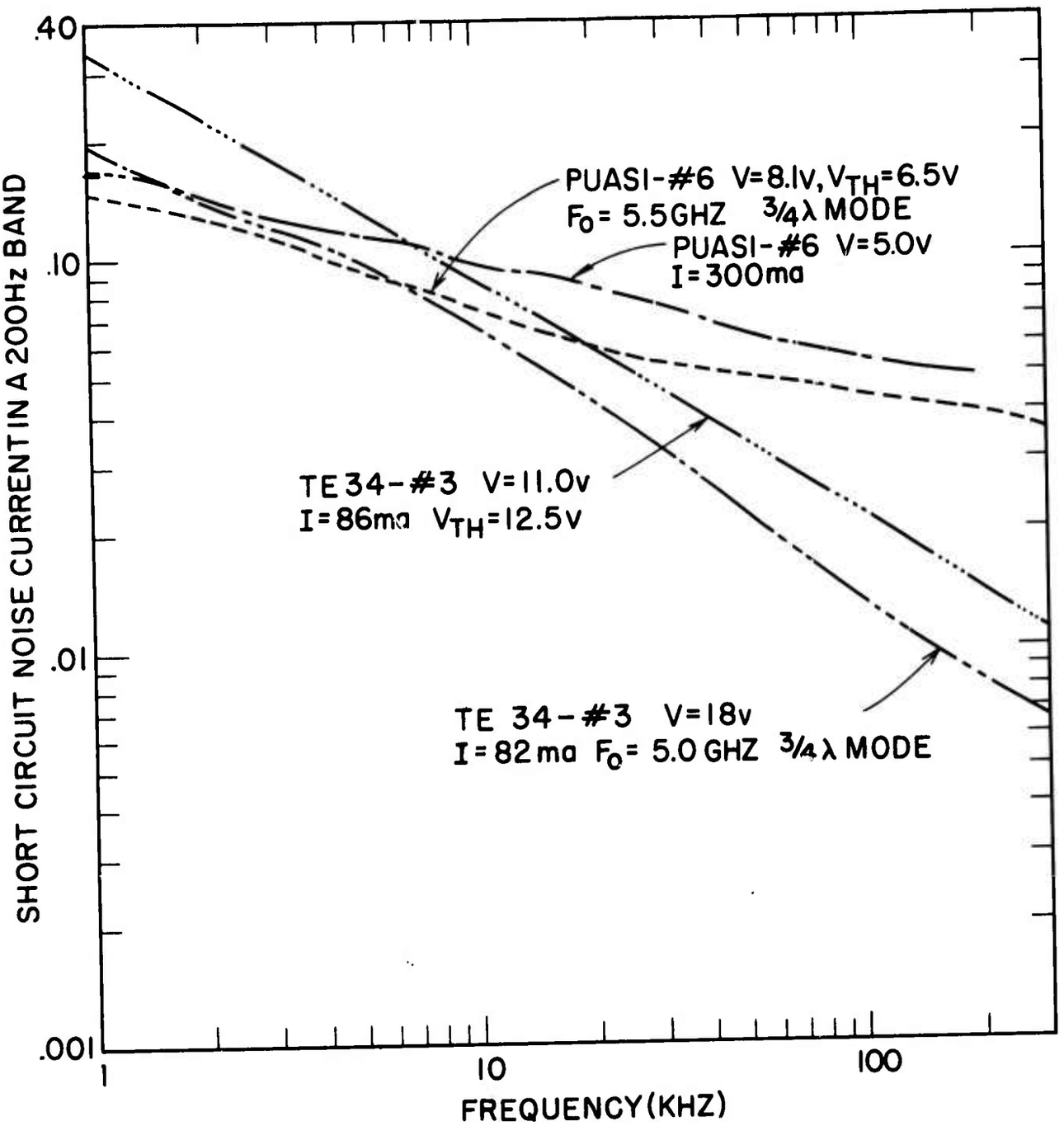

FIGURE 12: Low Frequency Noise Current Spectra

utilizing the same contact procedure was used. The geometry is illustrated in Figure 13. However, a satisfactory alloyed contact could not be obtained with the new geometry. The metal contacts would not adhere well to the gallium arsenide in the hole and could be easily detached during routine measurements using a probe contact. Gunn oscillations did not occur for these devices in either CW or pulsed operation.

Threshold Variations with Temperature

From pulsed I-V measurements made at different temperatures, measurements have been made of the variation of the threshold current, I_{th}, and of the threshold voltage, V_{th}, with temperature between -17°C and 90°C. Above 90°C it increases with increasing temperature as shown in Fig. 14. The threshold current increases with increasing temperature over the entire temperature range.

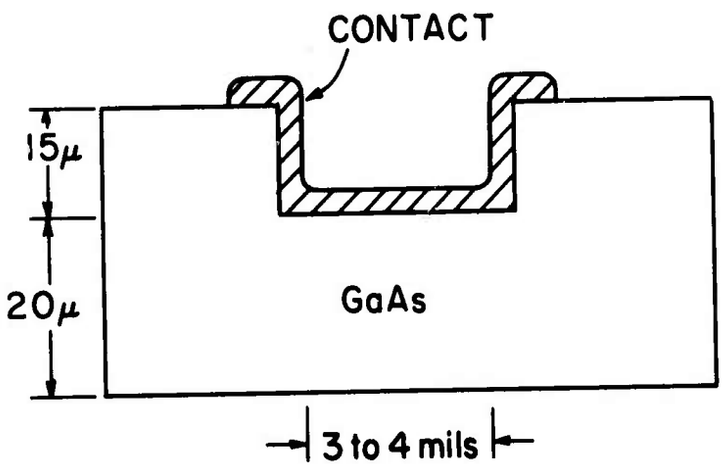

FIGURE 13: Gunn Device "Hole Configuration"

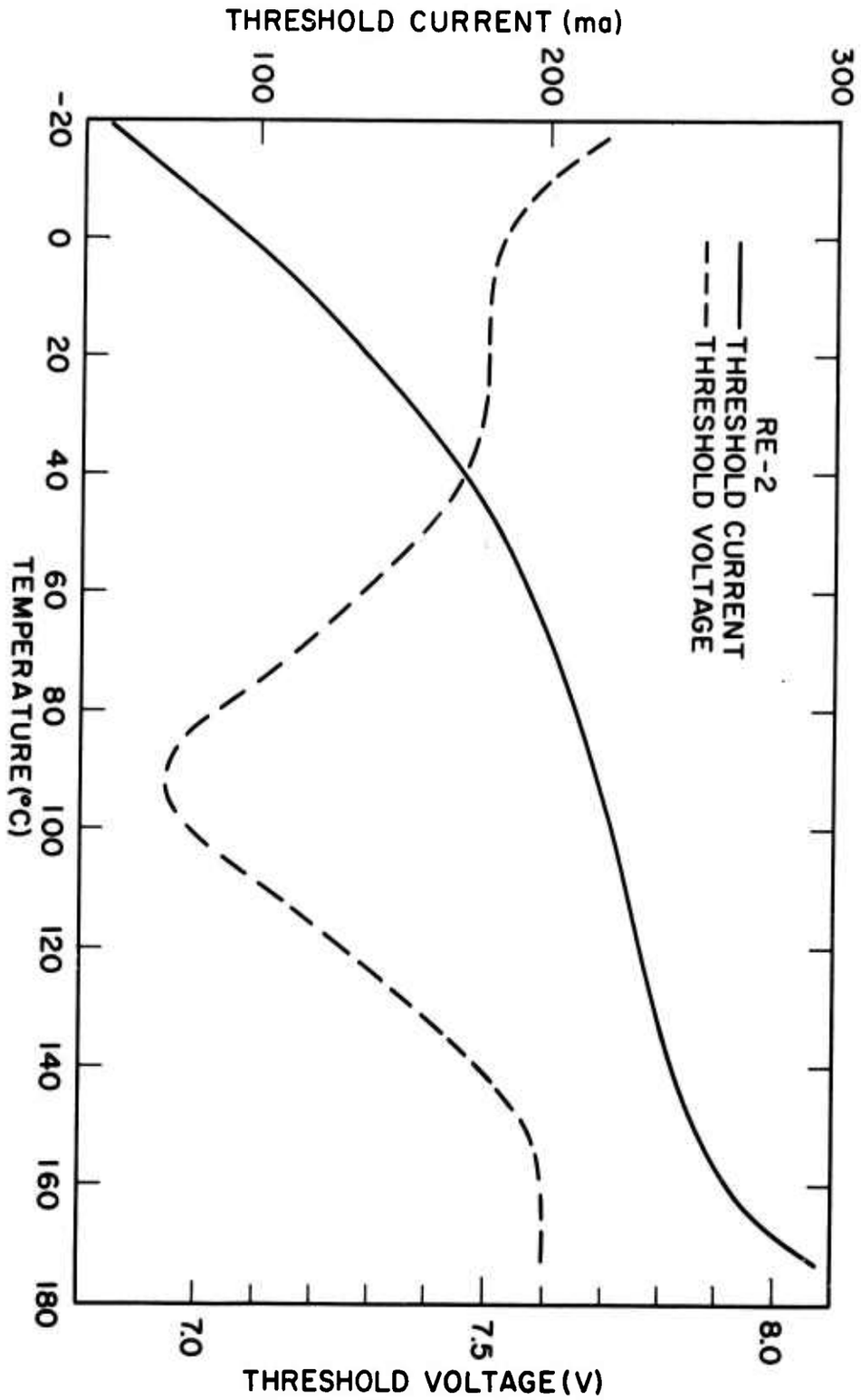

FIGURE 14: Temperature Behavior of Threshold Voltage and Current

II. COMPUTER CIRCUIT SIMULATION OF THE GUNN DEVICE

II. 1 Introduction

When homogenous devices of n-type GaAs with ohmic contacts are subjected to high d.c. bias fields, coherent microwave oscillations have been observed[1]. The current in a low-resistance circuit connected between the bias supply and the device has been found to consist of current pulses with a characteristic period. Capacitive probe measurements by Gunn[2] and Heeks[3] have shown that the current oscillations arise from the uniform drift through the device of narrow, high-field domains with equal low fields on either side. The characteristic period is the transit time of the high-field domain if it is assumed that the domain nucleation and its full formation at the source contact and its decay at the drain contact take place in a time very small compared to the domain transit time. In this report, a simple computer model for the domain behavior is proposed and some preliminary results, obtained from the computer experiments, are presented.

A very general and complicated problem of assuming boundary conditions in time and space and following the formation, transit and decay of the domains has been considered by McCumber and Chynoweth[4]. Their computer calculations show that the high-field domains form at the source contact, grow as they move toward the drain contact and remain stable in shape until they near the drain contact. Copeland[5], using McCumber-Chynoweth model, treated stable-domain propagation with diffusion coefficient D as a

function of electric field. His calculations clearly showed that as the applied voltage is increased, the current decreases implying that the device as a whole looks like a negative resistance while a domain is present.

II.2 Domain Properties

The bulk J-E characteristic of n-type GaAs is shown in Fig. 15. Typically E_{th} = 3.2 kV/cm, E_V depends largely on the purity of the material and is between 10 and 100 kV/cm; J_P/J_V = 2.

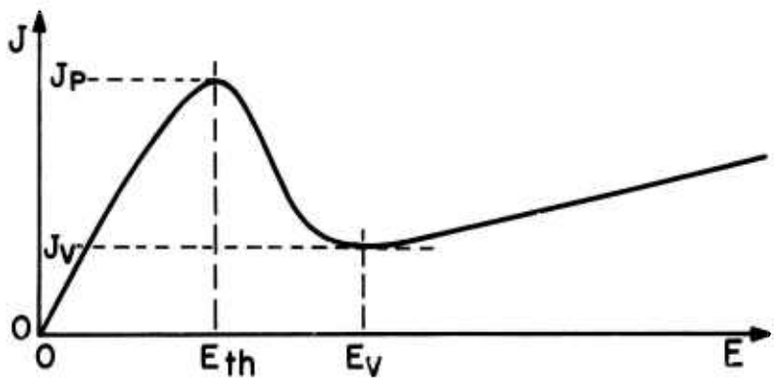

FIGURE 15: J-E Characteristic of a homogenous n-type GaAs sample

We would experimentally observe this curve if the device is homogenous and if the electric field is uniform in the sample. However, as soon as the applied voltage is increased to a value that makes $E \geq E_{th}$, a high-field domain is nucleated at the source contact resulting in a drop in electric field outside the domain. Because of the negative differential mobility for $E_{th} \leq E \leq E_V$, the domain rapidly builds up causing a further decrease in electric field outside the domain and hence the bulk current. If the device voltage is assumed to remain constant, the build-up continues until the electric field in the domain is above the negative differential mobility range. This is what we mean by a mature or fully-formed domain. The fully-formed domain then drifts out into the drain contact without undergoing changes in shape and in the value of electric field. The domain properties can best be represented by an $E_1 - V_D$

characteristic which is derived by Copeland[5] from his computer calculations. E_1 is the electric field in the bulk outside of the domain and V_D is the excess voltage of the region occupied by the domain. As the domain voltage increases, the outside electric field, and hence the bulk current, decreases resulting in a negative differential resistance for the domain.

II. 3 Computer Model of the Domain and the Device

The device to be simulated on the computer is shown in Fig. 16 where L_S is the length between contacts of the Gunn device and w_d is some average value for the domain width which is usually a function of the bias voltage, length of the device and the doping level. For long devices, $w_d << L_S$.

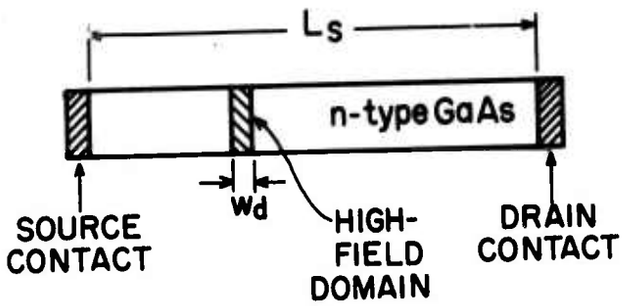

FIGURE 16: Device System to be Simulated

Since most of the experimental Gunn devices used in this Laboratory have low-field resistivities of about 1 ohm-cm, a first simulation attempt is made with the domain E_1-V_D curve corresponding to a doping level of 10^{15}/cc. A piece-wise linear approximation to this curve by five segments is shown in Figure 17 as I_{RD} - V_D curve, where $I_{RD} = en_oA\mu_1E_1$; e is the electron charge and μ_1 (= 5000 cm^2/V sec) is the electron mobility in the lower conduction band of n-type GaAs. The active device area A is taken as 0.71×10^{-4} $(cm)^2$. The curve marked 1 has a slope G_1 which is the inverse of the low-field

resistance of a device length w_d supposedly occupied by the domain. When the domain voltage exceeds $V_{th} \times w_d/L_S$, the part of the device in w_d becomes "active" and begins to form a high-field domain along curves 2 to 5. If the voltage across the device remains unchanged above the bulk threshold voltage V_{th}, a mature domain will be formed, with the outside bulk voltage dropping below V_{th}. The mature domain then drifts out into the drain contact with a velocity v_d given by

$$v_d = v_c (1 + c) \tag{1}$$

where v_c is the velocity of conduction electrons outside the domain and c is the fractional excess velocity of the domain over the outside electrons; Copeland estimates a value of 0.1 - 0.15 for c corresponding to $n_o = 10^{15}$. It should be noted that v_c depends on the outside electric field and hence the domain voltage. As the high-field domain begins to decay into the drain electrode, the outside bulk voltage begins to rise and correspondingly the voltage across the now-inactive part of the device w_d previously occupied by the decaying domain also increases and eventually exceeds its critical value V_{cl}. Thus a new domain is formed and is building up even as the old domain is moving out and the cycle of events repeats itself as a function of time. The above discussion suggests both a voltage-dependent and time-dependent equivalent circuit for the domain and an independent equivalent circuit for the bulk outside the domain as shown in Figure 18.

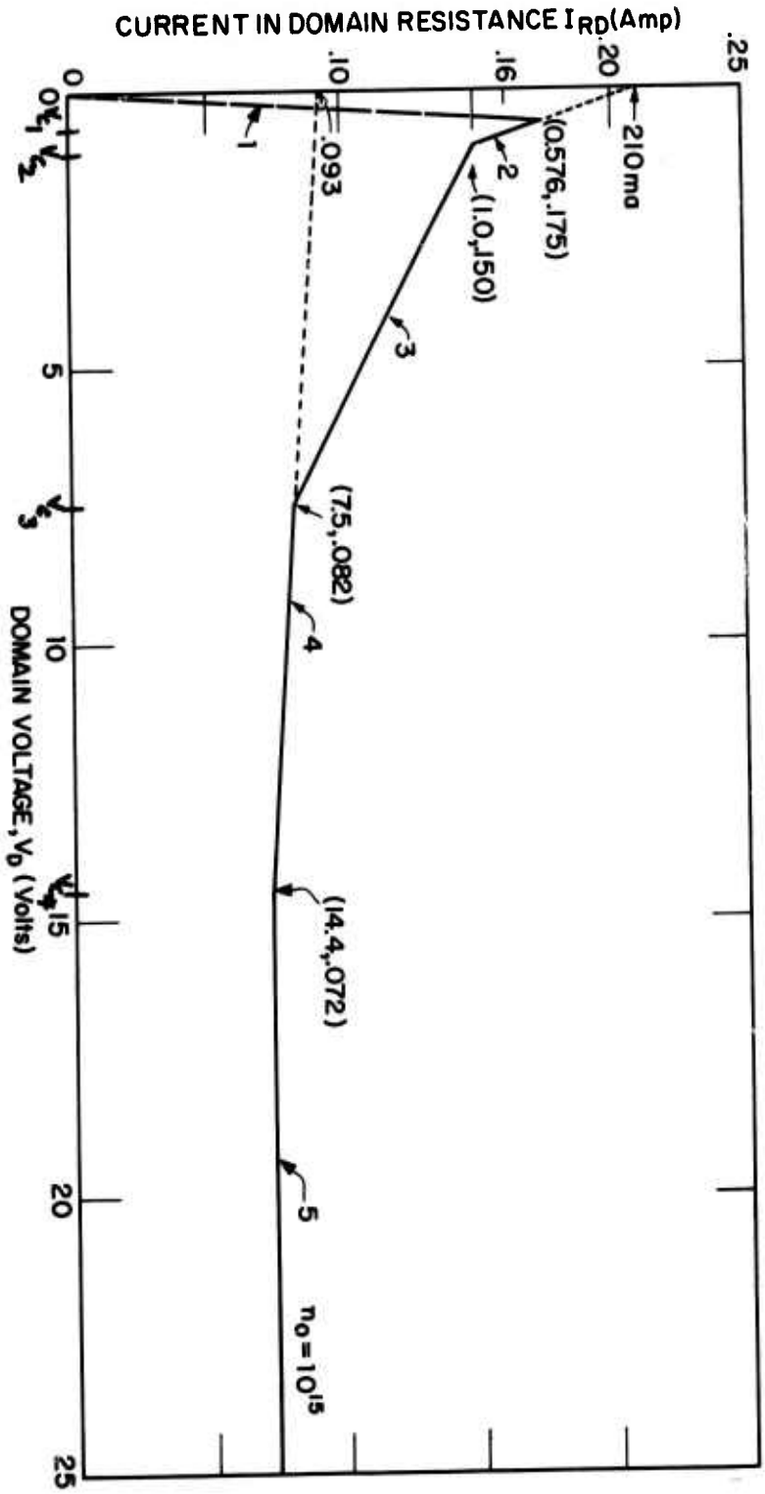

FIGURE 17: Linear Approximation to Domain V-I Characteristic

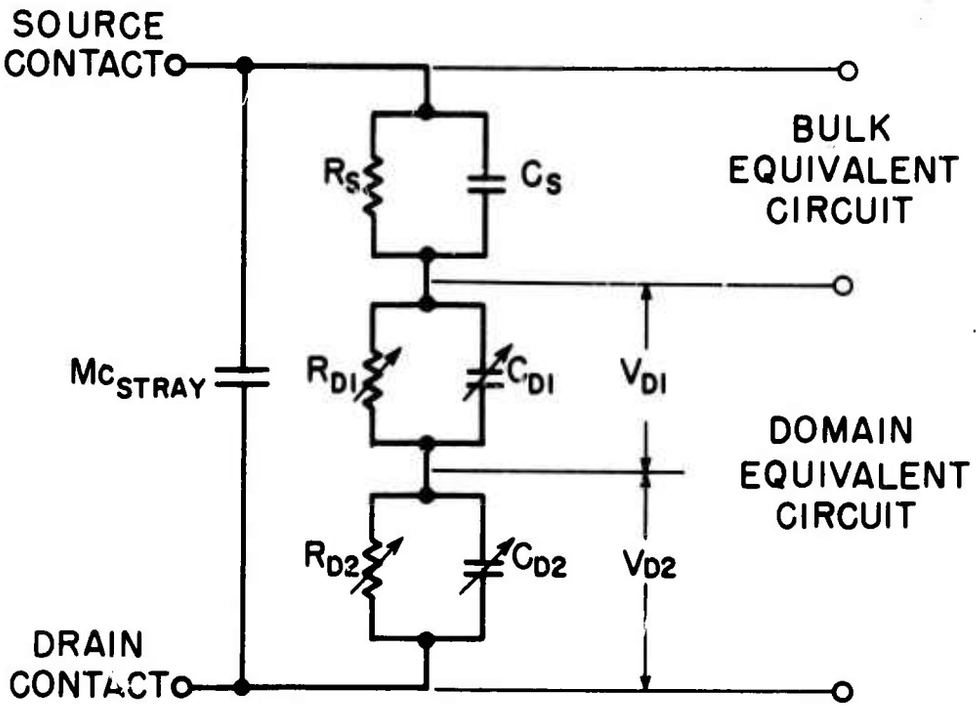

FIGURE 18: Equivalent circuit of the domain and the bulk outside of the domain

The algebraic symbols appearing in the equivalent circuit have the following significance:

R_S - Low-field resistance of the bulk material of length $(L_S - 2\ w_d)$ outside the domain

C_S - Electrostatic capacitance of the bulk material of length $(L_S - 2\ w_d)$

C_{Stray} - Stray capacitance of the package on which the device is mounted

$R_{D1,2}$ - Resistances of the active and/or inactive domains of voltages V_{D1} and V_{D2} as determined from the slopes in Fig. 17.

$C_{D1,2}$ - Voltage dependent capacitances of the active and/or inactive domains similar to p-n junction capacitance and expressed for accumulation and fully depleted regions as

$$C_{D1,2} = \frac{A}{2} (2 \epsilon q n_o)^{1/2} (V_{D1,2})^{-1/2} \quad (2)$$

where A is the active device area:

ϵ is the relative dielectric constant of the bulk material, and

q is the electron charge.

For $V_{D1,2} \leqslant V_{C1}$, the domain capacitance should approach the electrostatic capacitance of the device of width w_d given as

$$C_D = \frac{\epsilon A}{w_d} \quad (3)$$

(2) and (3) provide useful information about the domain width w_d corresponding to a domain critical voltage V_{C1}.

II. 4 Formulation of the Problem for Computer Calculations

A general network consisting of two parallel resonant circuits connected in series with the bias supply and the device can be made to look like a pure resistive load or a series combination of resistor and inductor or any other desired combination of basic network elements. The general microwave network and the device equivalent circuit connected to the bias supply are shown in Fig. 19. Also shown are the nodes 0-4 and the reference node r.

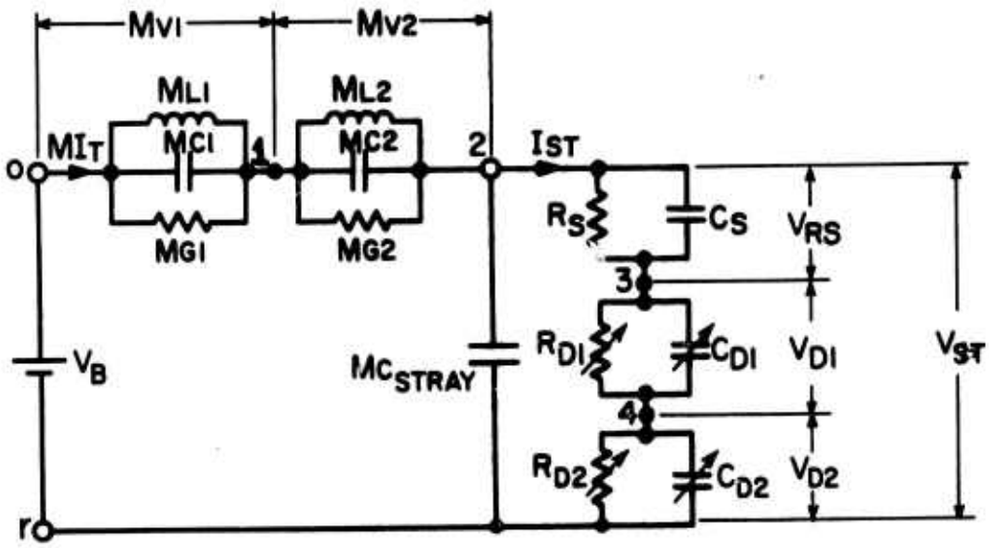

FIGURE 19: General Network - Device Programmed for Computer Calculations. The Voltage of node "O" with respect to the reference node r is the bias voltage V_B.

The basis of the calculations is that all the inductors and the capacitors can be converted to the equivalent combinations of resistors with current and voltage generators in a small time interval Δt which is very small compared to the smallest time constant in the microwave network - device system. For small intervals Δt, the following relations for the differential and integral terms hold good for nodes m and n:

$$\frac{d}{dt}\left(V_m - V_n\right) \approx \left[V_m\left(t_k + \Delta t\right) - V_n\left(t_k + \Delta t\right)\right] - \left[V_m\left(t_k\right) - V_n\left(t_k\right)\right] \quad (4)$$

$$\int \left(V_m - V_n\right) dt \approx \frac{\left[V_m\left(t_o\right) - V_n\left(t_o\right)\right]\Delta t}{2} + 2\sum_{t_k = 2}^{t_j} \frac{\left[V_m\left(t_k\right) - V_n\left(t_k\right)\right]\Delta t}{2} \quad (5)$$

where the subscripts o, k, j refer to the times corresponding to the running time variable from the time the computations began. Using (4), a capacitor

connected between nodes m and n can be replaced by the equivalent netowrk shown in Fig. 20 for the time interval Δt between t_k and $t_k + \Delta t$.

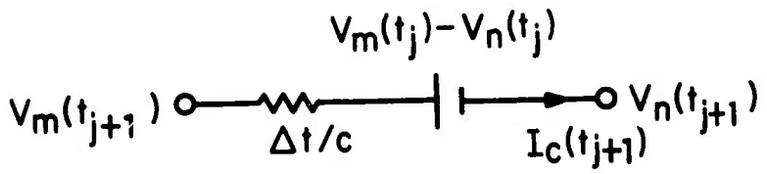

FIGURE 20: Equivalent Network Model of a Capacitor for Computer Calculations

The current flowing through the capacitor at time t_{j+1} is then related to the nodal voltages $V_m(t_j)$ and $V_n(t_j)$ at the end of time t_j and $V_m(t_{j+1})$ and $V_n(t_{j+1})$ as

$$I_C(t_{j+1}) \approx \frac{c}{\Delta t}\left[\left\{V_m(t_{j+1}) - V_n(t_{j+1})\right\} - \left\{V_m(t_j) - V_n(t_j)\right\}\right] \qquad (6)$$

Similarly, using (5), an inductor between nodes m and n can be replaced by the computer model shown in Fig. 21. The currents $I_L(t_j)$ and $I_L(t_{j+1})$ can be related to the old and new nodal voltages as

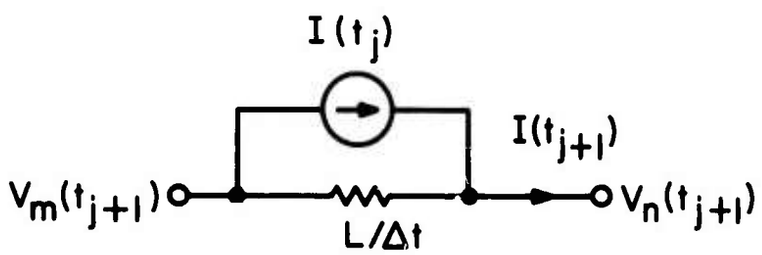

FIGURE 21: Computer model of an inductor for the time interval Δt between t_j and $t_j + 1$

$$I_L(t_j) \approx I_o + \frac{\left[V_m(t_o) - V_n(t_o)\right]\Delta t}{2L} + 2\sum \frac{\left[V_m(t_k) - V_n(t_k)\right]\Delta t}{2L} \quad (7)$$

$$I_L(t_{J+1}) \approx I_L(t_j) + \frac{\left[V_m(t_{j+1}) - V_n(t_{j+1})\right]\Delta t}{2L} \quad (8)$$

where I_o is the inductor current at the beginning of the computation cycle.

The computer model of a resistor is obviously simple and the current $I_R(t_{j+1})$ flowing through a resistor connected between nodes m and n is given as

$$I_R(t_{j+1}) = \frac{\left[V_m(t_{j+1}) - V_n(t_{j+1})\right]}{R} \quad (9)$$

Equations (6) - (9) allow us to draw a computer model of the general network - device system shown in Fig. 19 for a time interval Δt between times t_j and t_{j+1}. The computer model will consist of only resistors, voltage sources and no reactive elements. The standard nodal analysis is used to determine the new nodal voltages at t_{j+1} in terms of the old nodal voltages and the voltage and current sources at t_j. The new voltage and current sources can be determined from (6) - (9) and the whole computation cycle is repeated for the next time interval Δt.

The real voltages of interest, MV1, MV2, V_{ST}, V_{RS}, V_{D1} and V_{D2}, can be readily determined from the nodal voltages. I_{ST} and M_{IT} are the device current and the total microwave current, respectively. When V_{D1} (V_{D2}) exceeds any of the critical voltages V_{C1}, V_{C2}, V_{C3} and V_{C4} shown in Fig. 17, then R_{D1} (R_{D2}) changes states into a parallel combination

of a resistor and a current source. The value of the resistor is the inverse of the slope of the curve in Fig. 17 and the current source is the intersection of the curve on the current scale. The distance ΔL_d travelled by the active domain in Δt is given as

$$\Delta L_d = v_d \, \Delta t \tag{10}$$

where v_d is as given in (1). The velocity of conduction electrons outside the domain is given as

$$v_c = \frac{I_{RS}}{q A n_o} \tag{11}$$

where I_{RS} is the value of current flowing in the bulk resistance outside the domain and is known as a function of time from the computer calculation of V_{RS}. This accounts for the variable domain velocity as the domain is building up and as it disappears into the drain contact. When the domain travel equals or slightly exceeds the device length L_S, then the domain resistance is switched back to state 1 corresponding to the positive resistance R_1 which is the inverse of the slope of curve 1 in Fig. 17. The current through R_{D1} (R_{D2}) is limited to the peak bulk current after the switching has taken place.

The choice of initial conditions at the beginning of the computation is important for a successful run of the program and for the attainment of steady state calculations. The initial conditions are chosen on the basis of a physically existing situation. Initially both V_{D1} and V_{D2} are equal and increase with time in the same way because C_{D1} and C_{D2} are the same and charge the

same way when the bias voltage is applied at t = O. At some time later when V_{D1} (V_{D2}) $\geq V_{C1}$, R_{D1} is allowed to switch to a negative resistance and a parallel current source corresponding to curve 2 in Fig. 17 while holding R_{D2} to a positive resistance of curve 1. If the voltage across the device remains above V_{th} and unchanged, C_{D1} now rapidly builds up voltage V_{D1} across it because it sees negative resistance along curves 2, 3 and 4 and an open circuit along curve 5. V_{D2} also increases above V_{C1} at a slower rate for some time because of the applied voltage, but it soon begins to decrease below V_{C1} because of the rapid increase in V_{D1} and because of the discharge of C_{D2} into the positive resistance R_1. As V_{D1} successively exceeds V_{C1}, V_{C3} and V_{C4}, C_{D1} varies according to (2) and R_{D1} switches to the parallel combinations of negative resistance and current source given by $(-R_2, I_2)$, $(-R_3, I_3)$, $(-R_4, I_4)$ and $(0, I_5)$, respectively. R_2, R_3 and R_4 are the inverse of the slopes of curves 2-4 and I_2, I_3, I_4 and I_5 are the intersections of curves 2-5 with the current axis in Fig. 17. When the distance travelled by the domain exceeds L_s, R_{D1} is switched back to R_1 causing C_{D1} to discharge rapidly and this situation corresponds to the domain disappearance into the drain contact. A fast decrease in V_{D1} will cause V_{D2} to increase and exceed V_{C1} after some time and a new "active" domain is triggered. These events repeat with V_{D1} and V_{D2} interchanging the roles of "active" and "inactive" domain voltages.

II. 5 Program Capabilities and Controls

The program at present has the capability of calculating the interaction of a microwave circuit with the Gunn device. The microwave

circuit may be a low or a high resistance; an inductor and a low resistance; a tuned circuit or a series combination of a tuned circuit and an inductor. A tuned circuit is a crude approximation to a cavity in which the Gunn device usually operates. A better approach will be to treat the cavity as a loaded transmission line in the time domain so as to bring the circuit in line with the device calculations. The program has the facility to do calculations in over 4000 time intervals of Δt, to print out and/or to plot to the desired accuracy the results obtained for V_{D1}, V_{D2}, V_{ST}, MV1, MV2, I_{ST} and M_{IT} as functions of time. The printing or plotting can be suppressed by controls read from a control card. At the end of a set of calculations or when the calculations diverge to an overflow situation, the computer program ceases doing any further calculations and gives out a diagnostic print-out of all the intermediary calculations which can be used to find sources of error or to feed in new initial conditions to continue calculations over another time period. When one wishes to continue calculations until steady state, these controls can be very helpful. A control character is used to control the punching of cards at the end of a specified computation period so that the set of punched cards can be used to resume computations at that point.

II. 6 Numerical Results

For a 1 ohm-cm n-type GaAs, $n_o = 10^{15}$/cc. The I-V curve of the domain for this doping level and for a device area of $0.71 \times 10^{-4}(cm)^2$ is shown in Fig. 17. The critical voltages can be read as $V_{C1} = 0.576$ v, $V_{C2} = 1.0$ v, $V_{C3} = 7.5$ v and $V_{C4} = 14.4$ v. From equations (2) and (3), a logical value for the domain width w_d is 1 micron. The pairs of resistance and

current source for curves 1-5 are obtained from Fig. 4 as (3.20, 0.0), (-15.67, 9.21), (-95.2, 0.16), (-714, 0.092) and (0.0, 0.072). If we choose a sample of L_S = 20 microns, the bulk resistance R_S is 32 ohms and the electrostatic capacitance C_S of the bulk is 0.05 pF. The inactive domain capacitance C_D is 0.9 pF corresponding to w_d = 1 micron. The value of stray capacitance due to the device package is given by M_{CS} = 0.28 pF. The fractional excess velocity c of the domain over the velocity of outside electron is taker to be 0.115. Several sets of computer runs have been made with this device equivalent circuit and for different bias voltages and microwave circuits. The time interval of computations Δt is chosen to be 1.5×10^{-13} second. They can be classified into two classes:

Class 1 a. The microwave circuit is a pure resistor of 1 ohm and the bias voltage is changed from V_{th} to 2 V_{th}.

b. The microwave circuit is a resistor of 5 ohms and the bias voltage is varied from V_{th} to 2 V_{th}.

Class 2 V_B = 10.5 V and the microwave circuit is a series combination of 1 ohm and an inductor of

a. 0.5 nH, b. 2.5 nH

Typical results of classes 1.a and 1.b are shown in Figs. 22-27 for a bias voltage of 10.5 volts. The switching between active and inactive domains can be clearly seen in Fig. 22. It may also be noted that the characteristic domain transit time is made up of a domain formation time, the transit time of a mature domain and the domain decay time. The domain formation time T_f is a significant part of the characteristic time T_G. Computer calculations

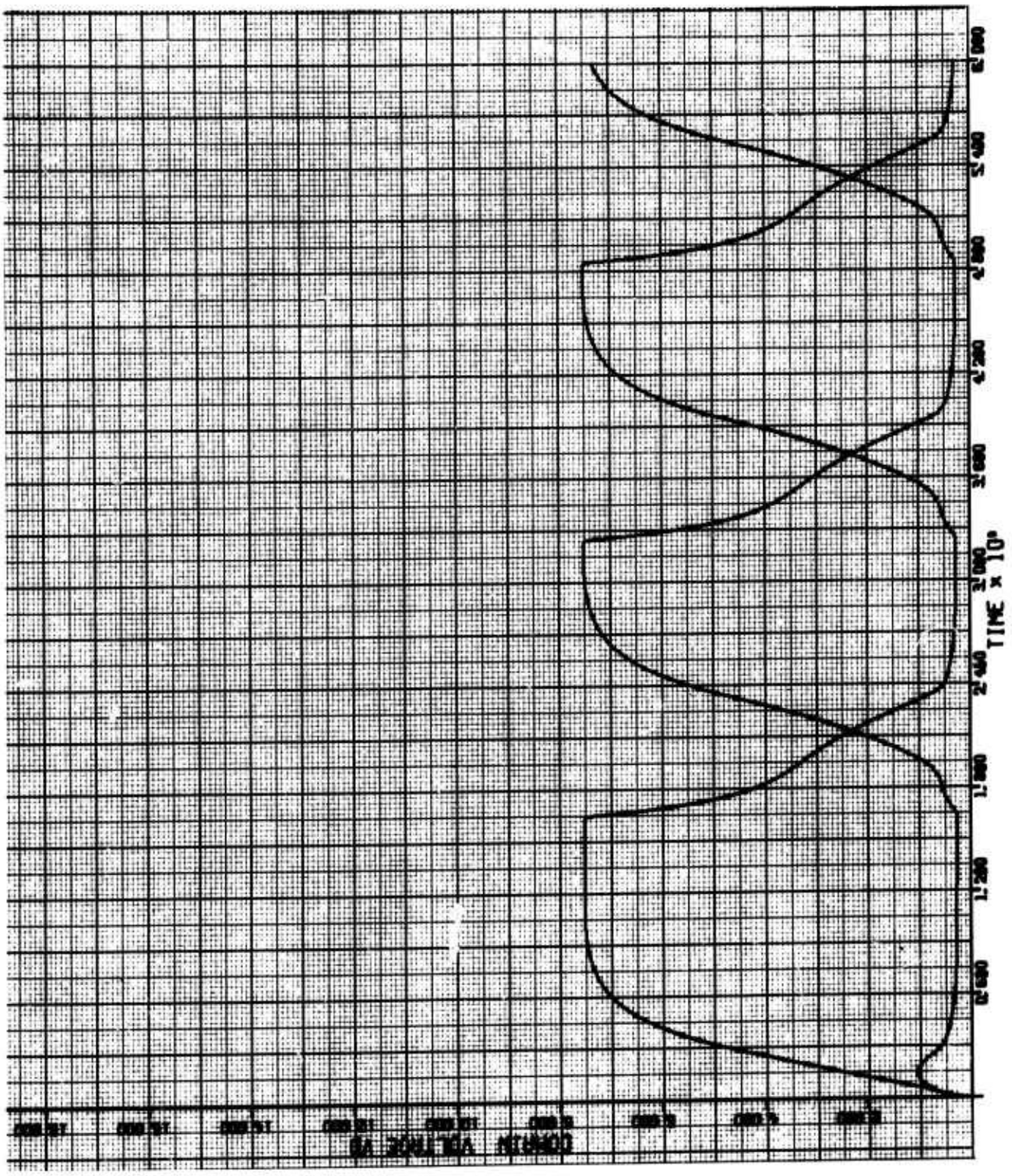

FIGURE 22: Domain Voltage for 1 Ohm Load

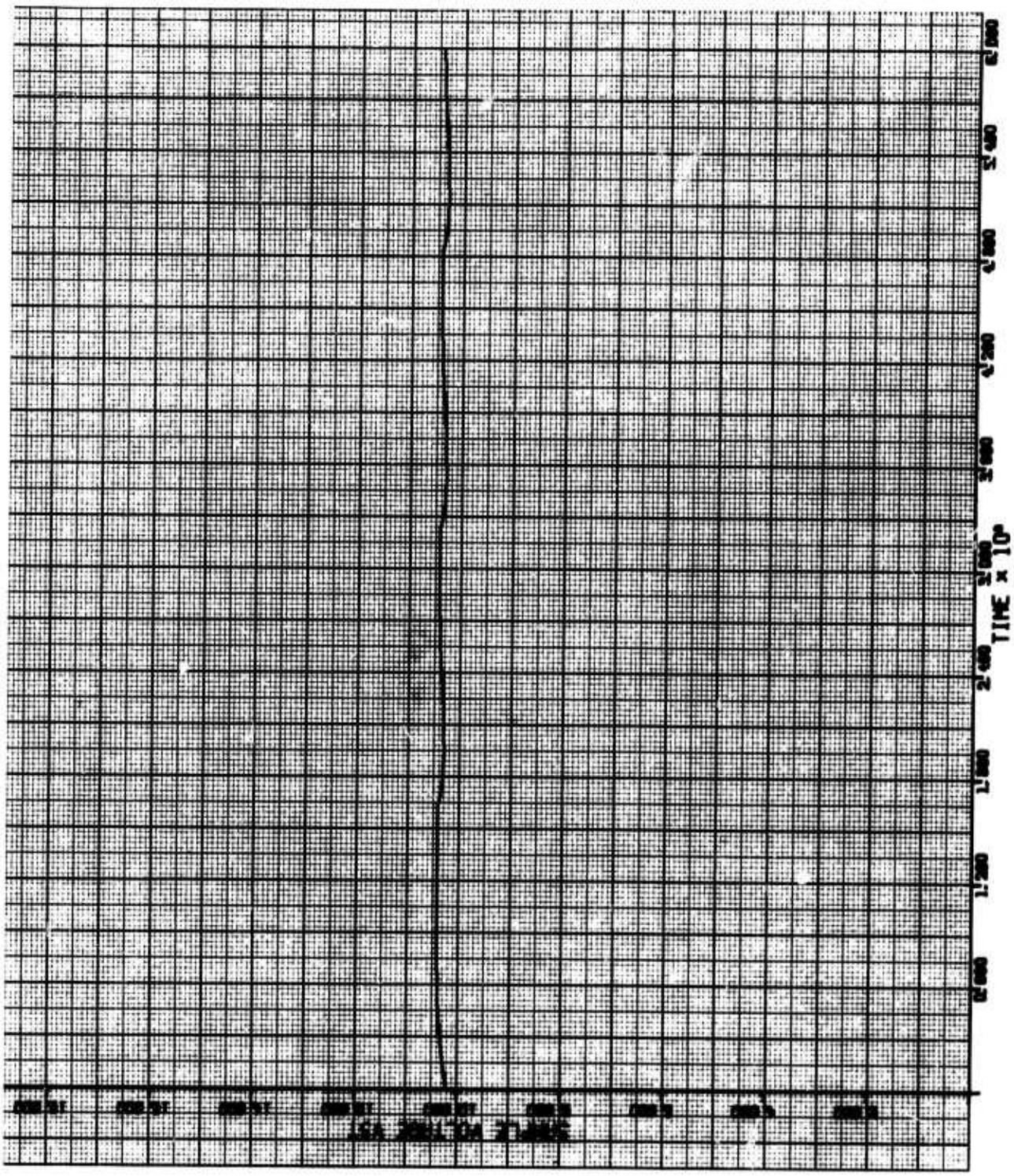

FIGURE 23: Device Voltage for 1 Ohm Load

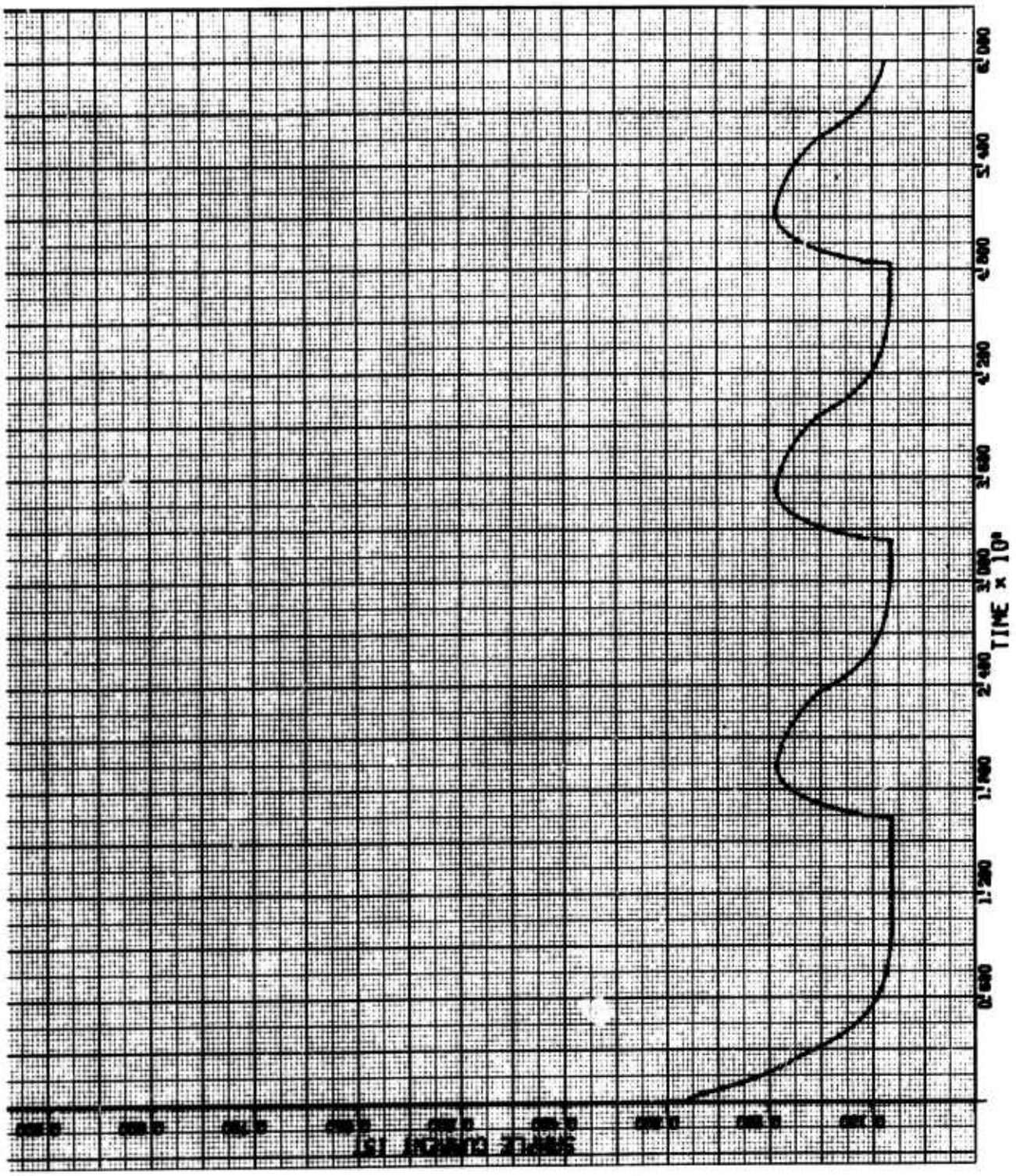

FIGURE 24: Device Current for 1 Ohm Load

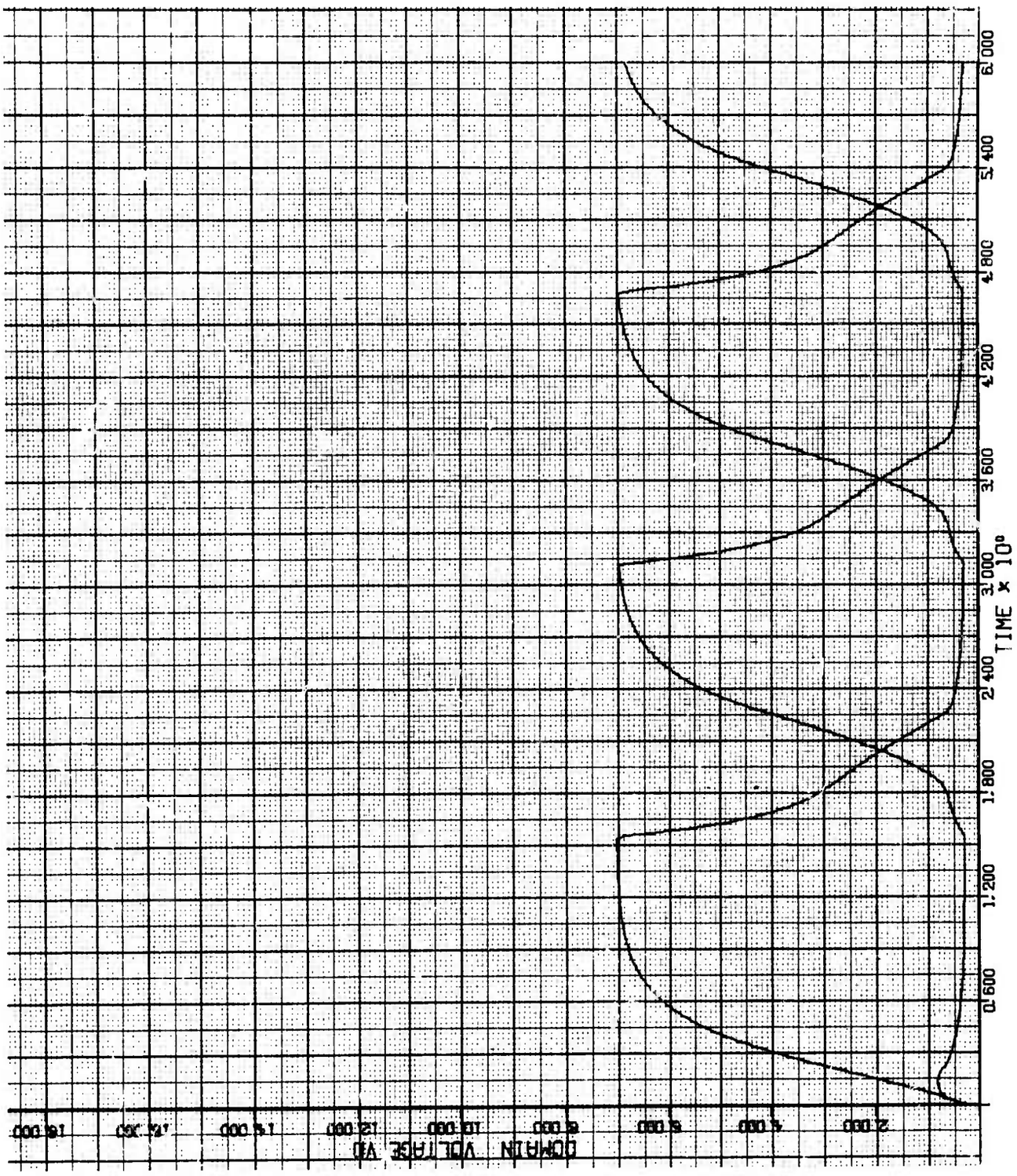

FIGURE 25: Domain Voltage for 5 Ohm Load

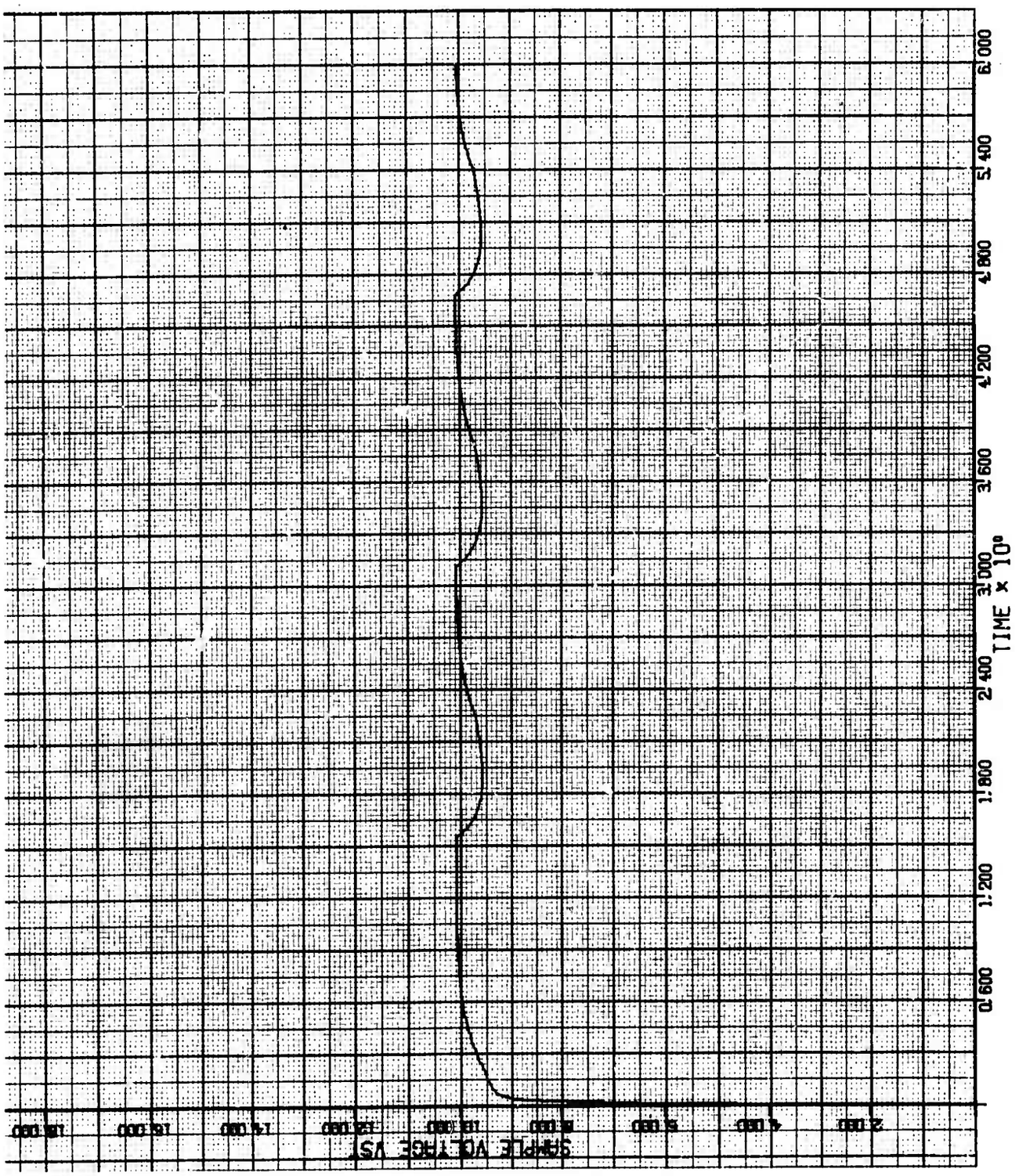

FIGURE 26: Device Voltage for 5 Ohm Load

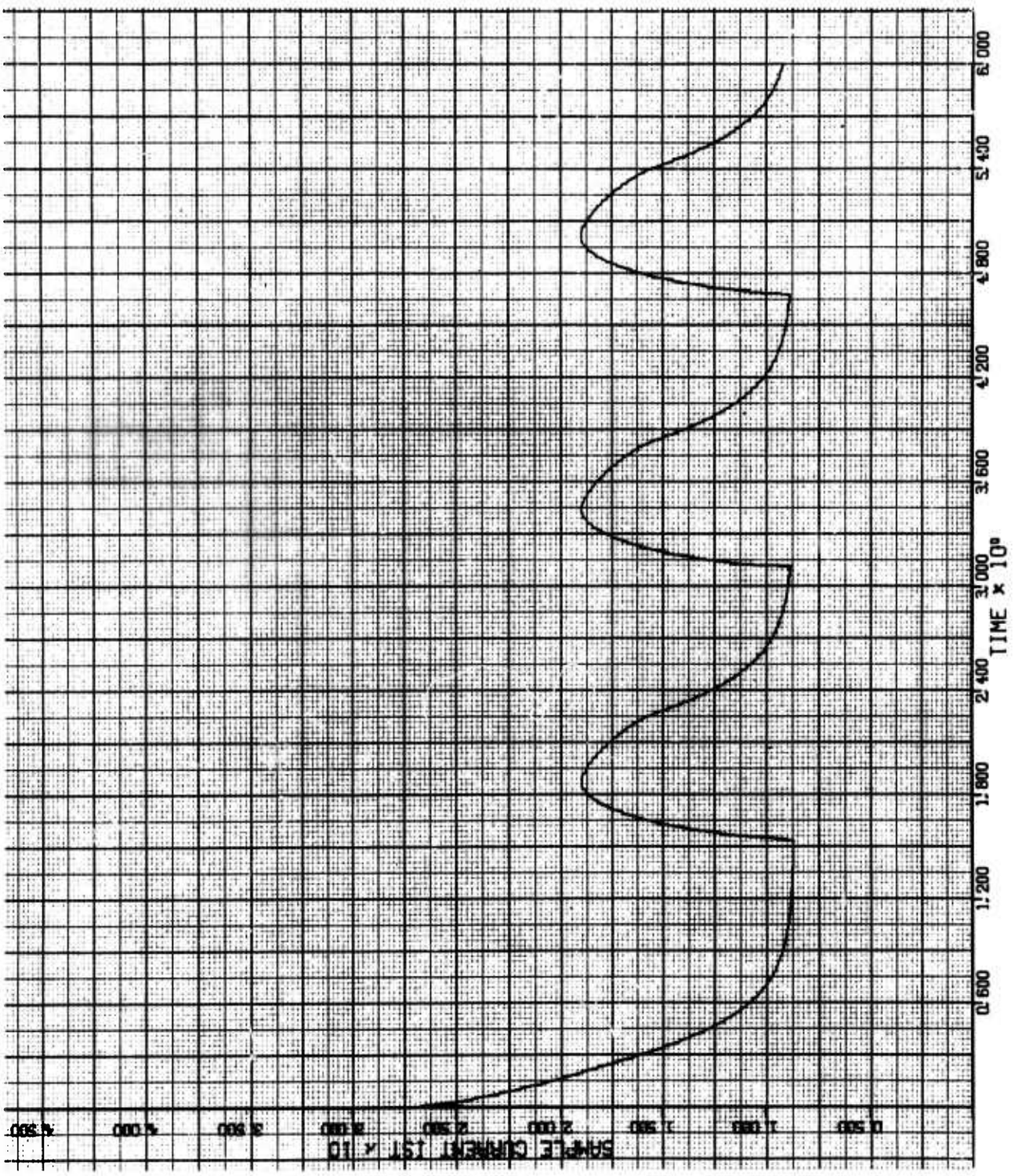

FIGURE 27: Device Current for 5 Ohm Load

indicate the T_f decreases with increasing bias voltage. It can also be seen from Figs. 22 and 25 that T_f increases with an increase in load resistor from 1 ohm to 5 ohms. The mature domain transit time T_{tr} is a lesser fraction of T_G and is found to increase with bias voltage. A comparison of Figs. 22 and 25 shows the decrease in T_{tr} as the load is increased from 1 ohm to 5 ohms. For large values of load resistance, T_G will be approximately the sum of domain formation and decay times. This can be explained by the fact that as the load resistor is increased, the voltage appearing across the device decreases and the domain is forced to grow with lesser device voltage and consequently takes a longer time to attain maturity. In this time, the domain would have travelled a significant portion of the sample and thus the mature domain has to travel only a small distance before it reaches the drain contact and begins to decay. The domain decay time T_d is not greatly influenced by either the bias voltage or the load resistance. Hence, the characteristic domain transit time T_G can be expressed as

$$T_G = T_f + T_{tr} + T_d \qquad (12)$$

The device voltage, shown in Figs. 23 and 26, is nearly constant for 1 ohm load and varies by about 0.5 V for the 5 ohm load. The device current, drawn as a function of time in Figs. 24 and 27, shows the kind of pulsed behavior experimentally seen by Gunn and others, with a peak to valley current ratio of about 2.25. It can be seen that the flat part of the current pulse is longer for the 1 ohm load because of the larger mature domain transit time than in the 5 ohm case. The negative resistance of the bulk device

in the presence of a high-field domain can be clearly seen from Figs. 23 and 24 and from Figs. 26 and 27 where an increase in device voltage V_{ST} reflects in a decrease in the device current I_{ST} and vice versa.

A characteristic frequency, also known as the Gunn frequency f_G, of the devices is the inverse of domain transit time T_G. The variation of f_G with bias voltage can be easily measured in the Laboratory using a device mount that operates into a resistive load. The Gunn frequency determined from the computer calculations for two values of load resistance as the bias voltage is changed from a value slightly above V_{th} to about $2\ V_{th}$ is shown in Figure 28. The Gunn frequency first decreases as the bias voltage is increased and then increases beyond a certain bias voltage. Gun frequency tuning of more than 15 per cent can be achieved by changing the bias voltage above V_{th} and these predictions are in good agreement with the experimental results obtained at this Laboratory.

The device voltage is nearly a constant when it is operated into small values of load resistance. However, the device voltage can show a large variation with time if an inductor is added in series with the 1 ohm resistance. The domain movement will now depend on both the transit time and the device voltage. The computer calculations of class 2 have been obtained for $V_B = 10.5$ V for two values of inductor, one a small value of 0.5 nH and the other of 2.5 nH. The computer plots of the results obtained with 0.5 nH are shown in Figs. 29 - 33 and those with 2.5 nH are shown in Figs. 34 - 38. A considerable swing of the domain voltage V_D ($V_{D1} + V_{D2}$), the device voltage V_{ST} and the voltage across the inductor M_{V2} may be noticed

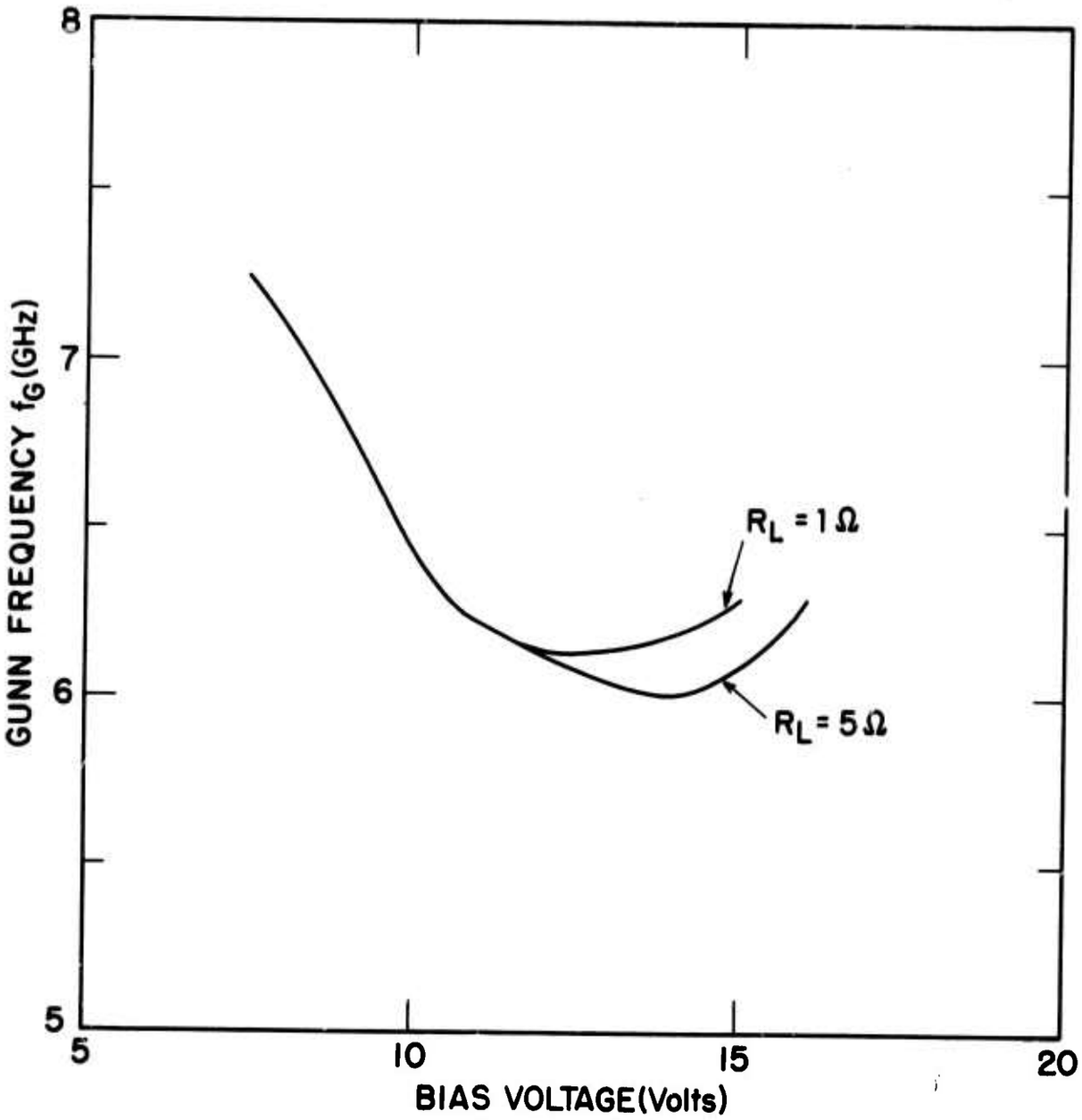

FIGURE 28: Calculated Gunn Frequency vs. Bias Voltage

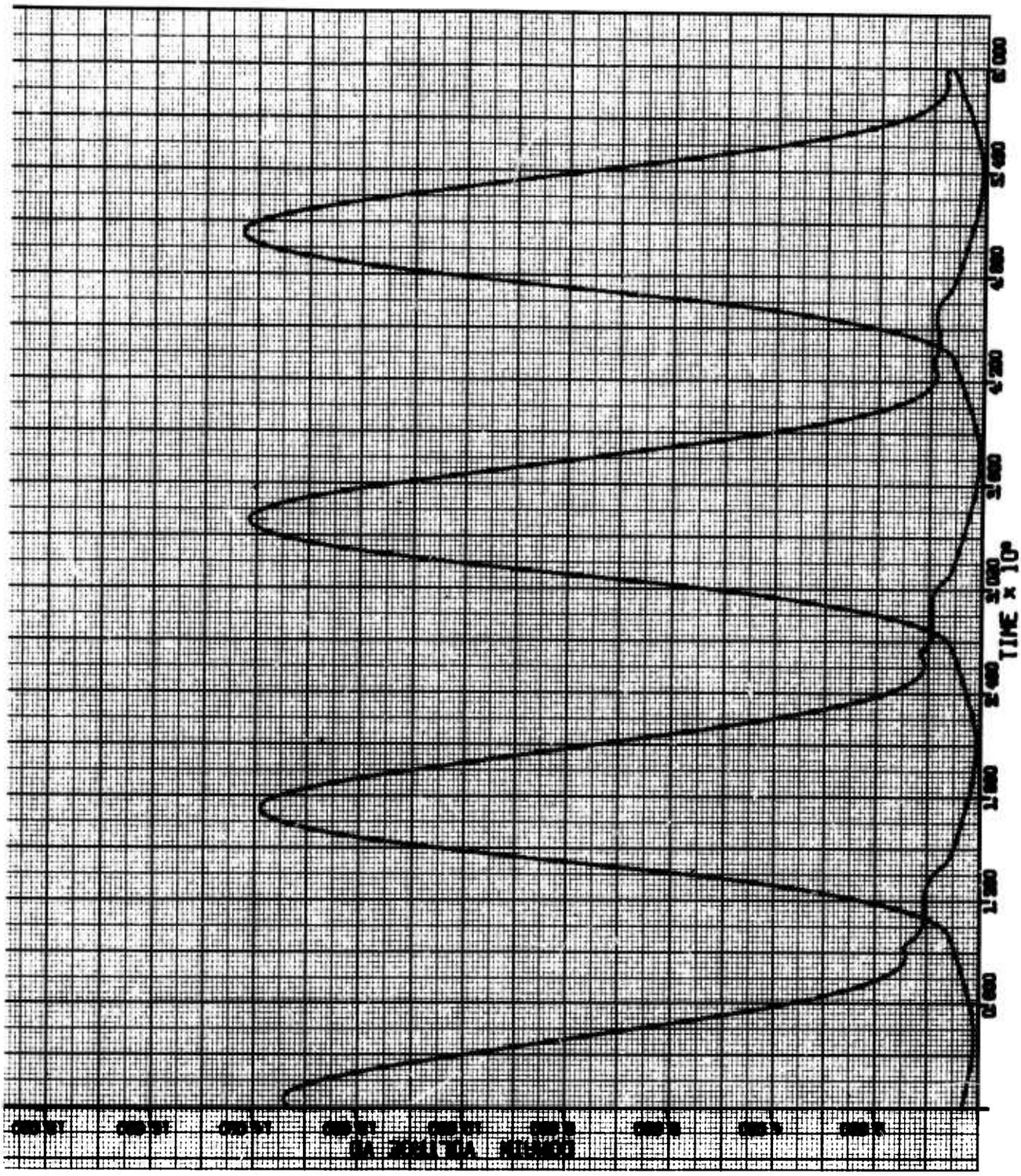

FIGURE 29: Domain Voltage for 1 Ohm and 0.5 nh Load

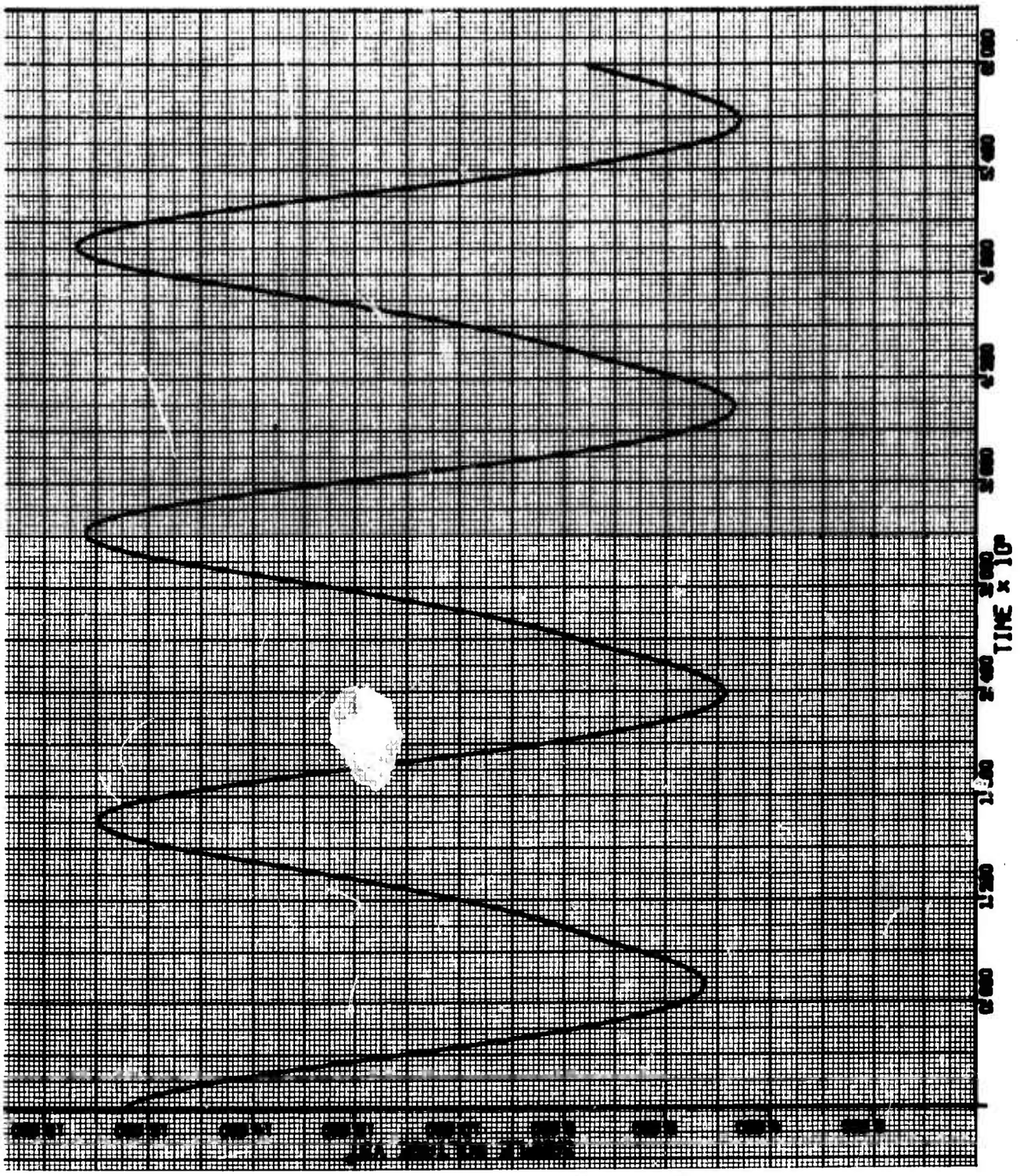

FIGURE 30: Device Voltage for 1 Ohm and 0.5 nh Load

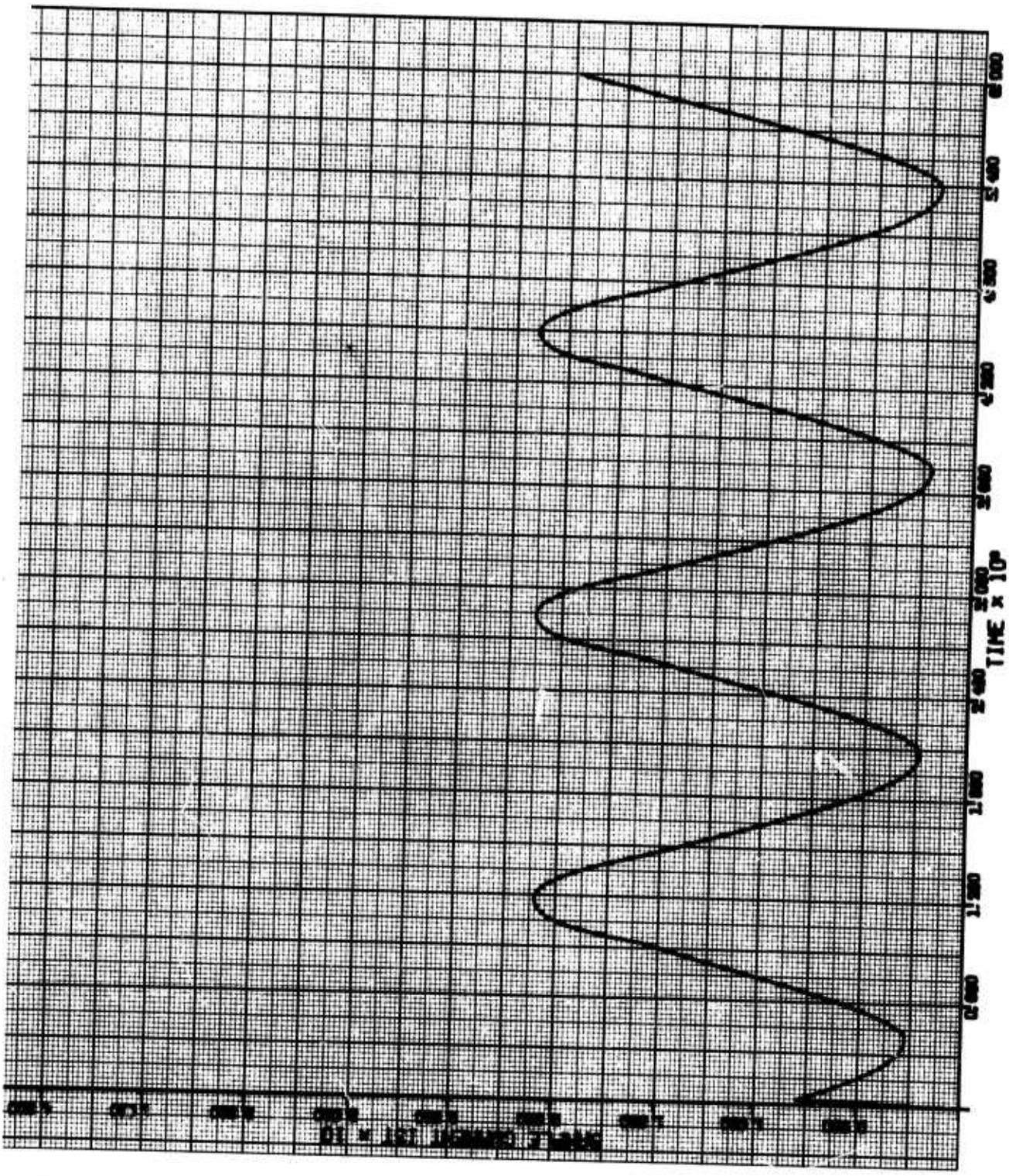

FIGURE 31: Device Current for 1 Ohm and 0.5 nh Load

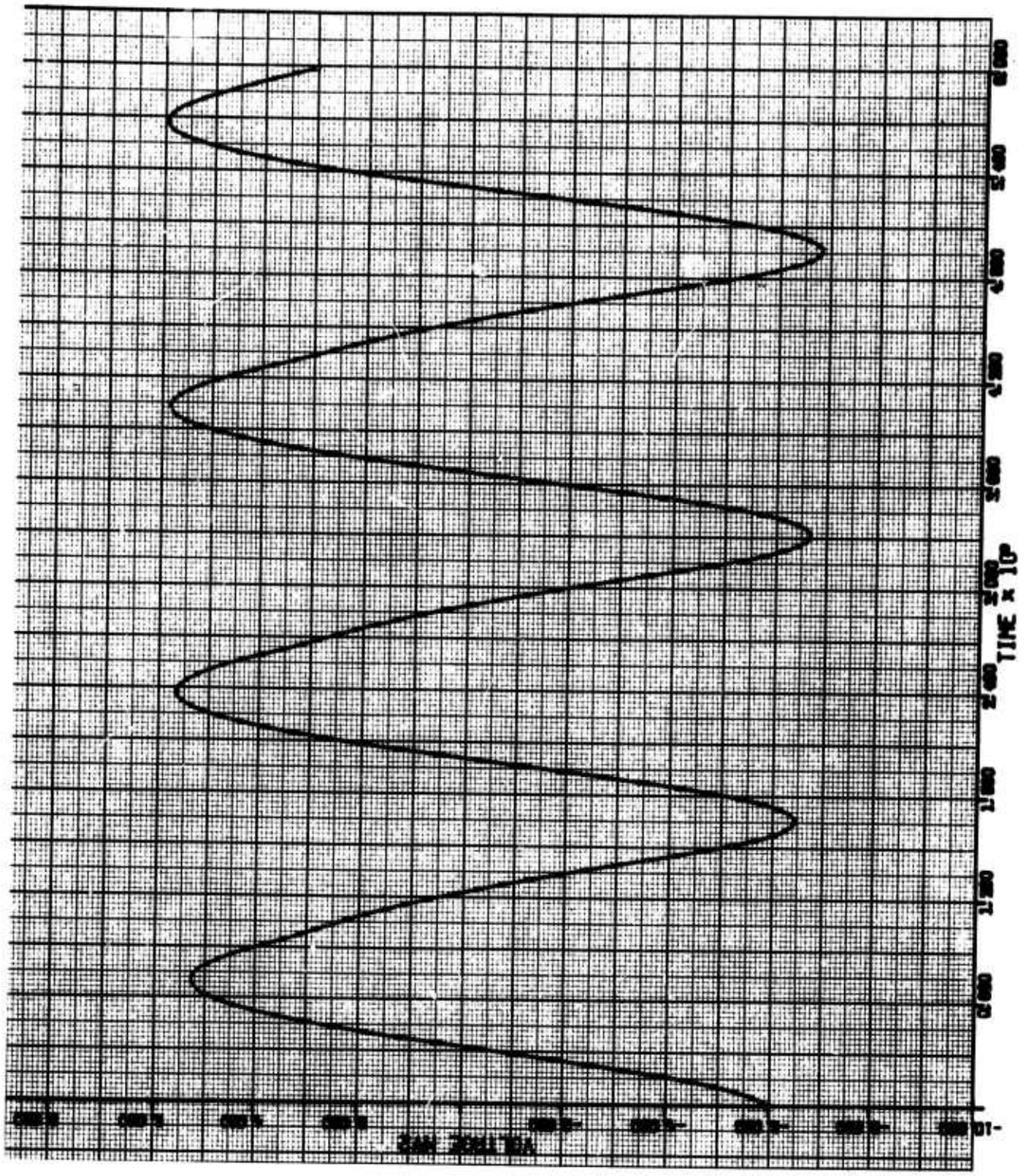

FIGURE 32: Inductor Voltage for 1 Ohm and 0.5 nh Load

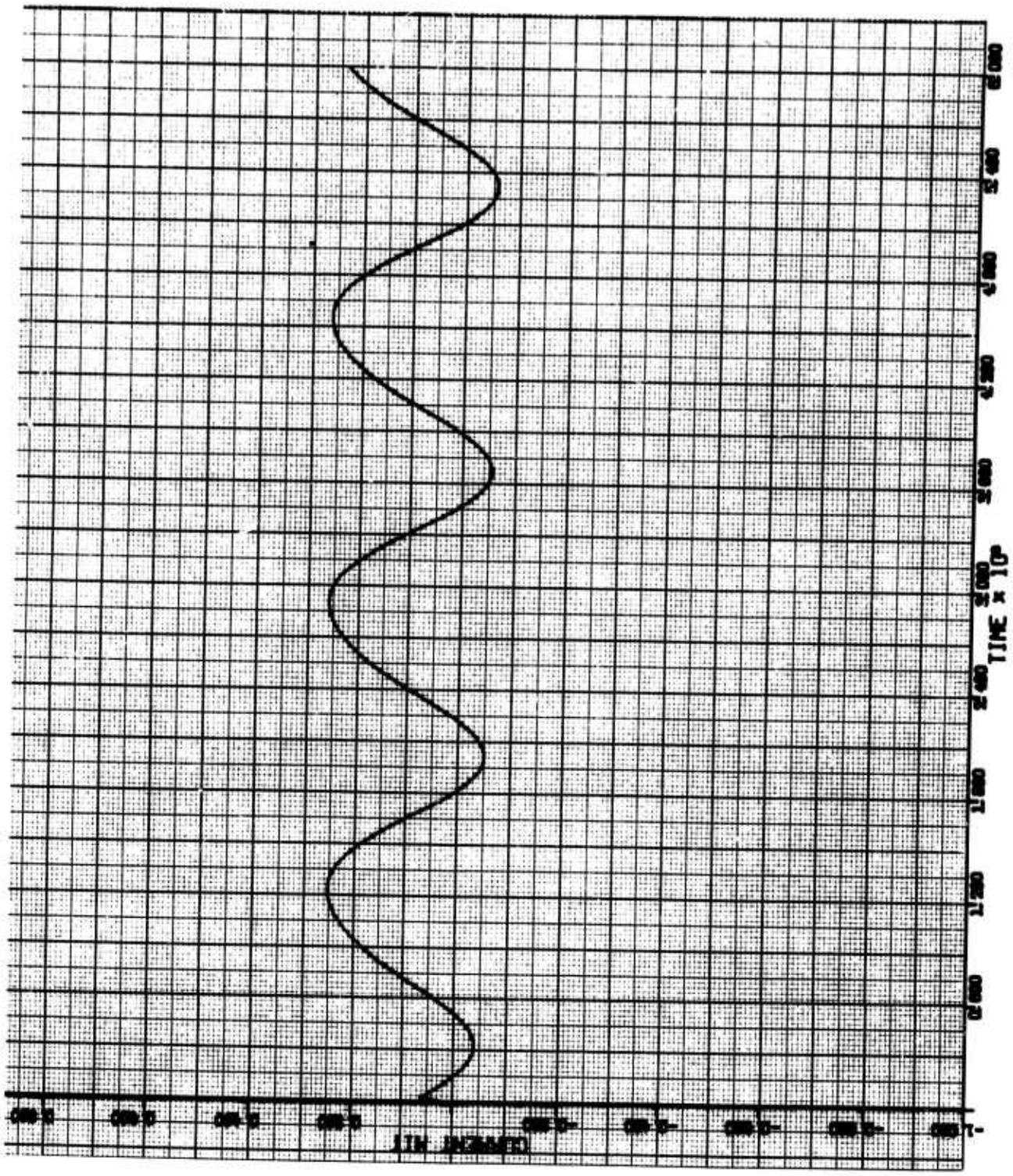

FIGURE 33: Microwave Circuit Current for 1 Ohm and 0.5 nh Load

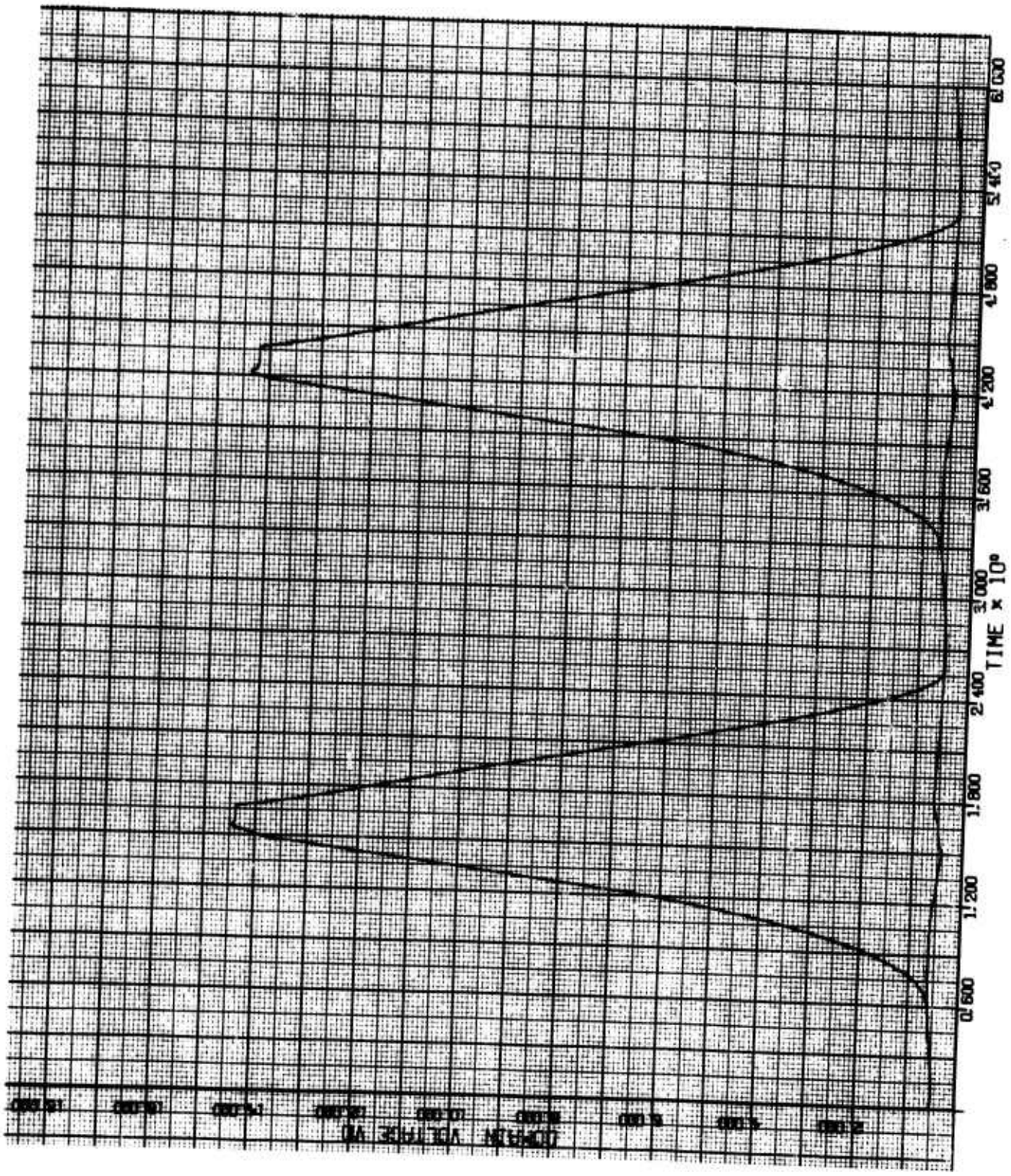

FIGURE 34: Domain Voltage for 1 Ohm and 2.5 nh Load

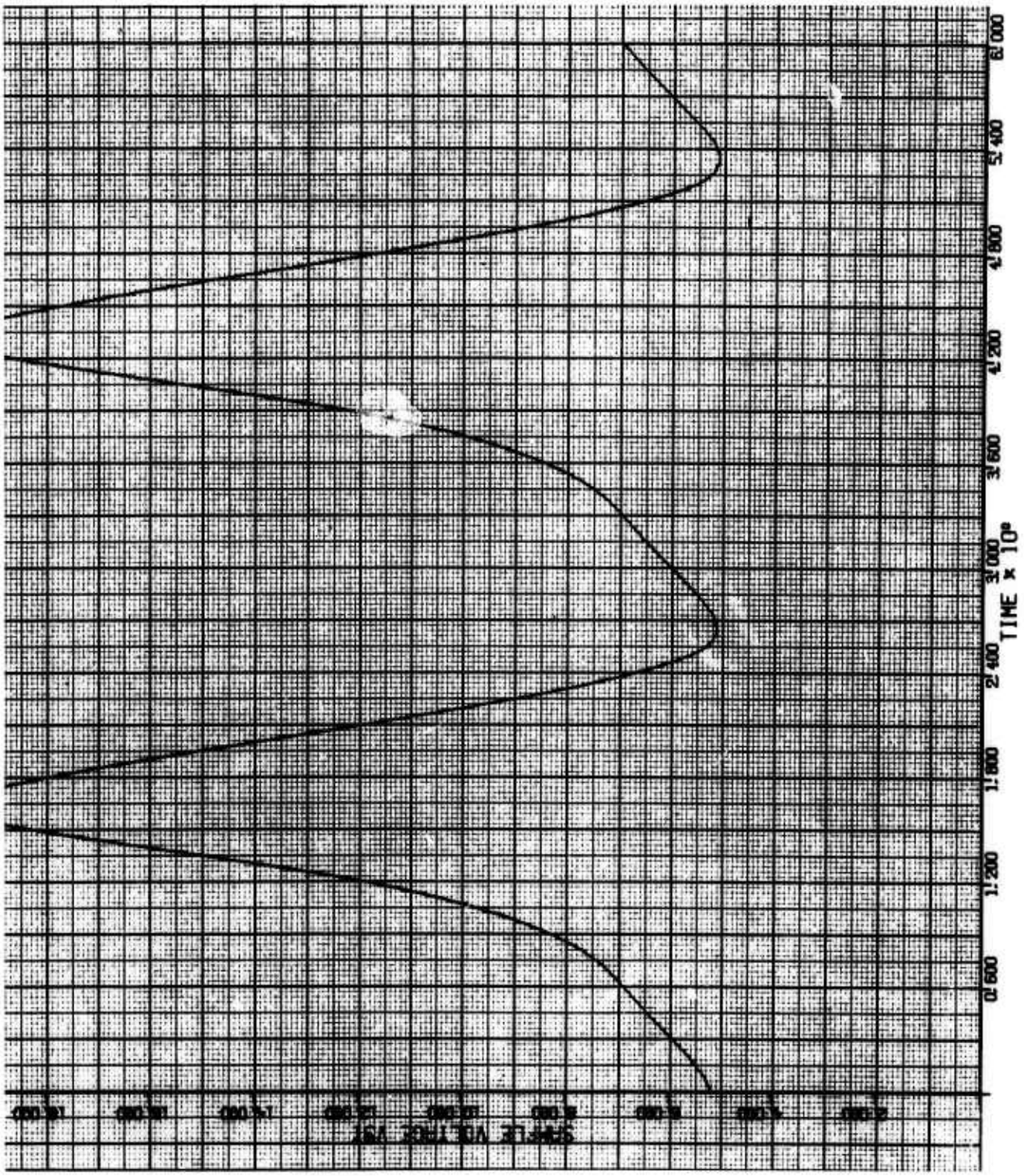

FIGURE 35: Device Voltage for 1 Ohm and 2.5 nh Load

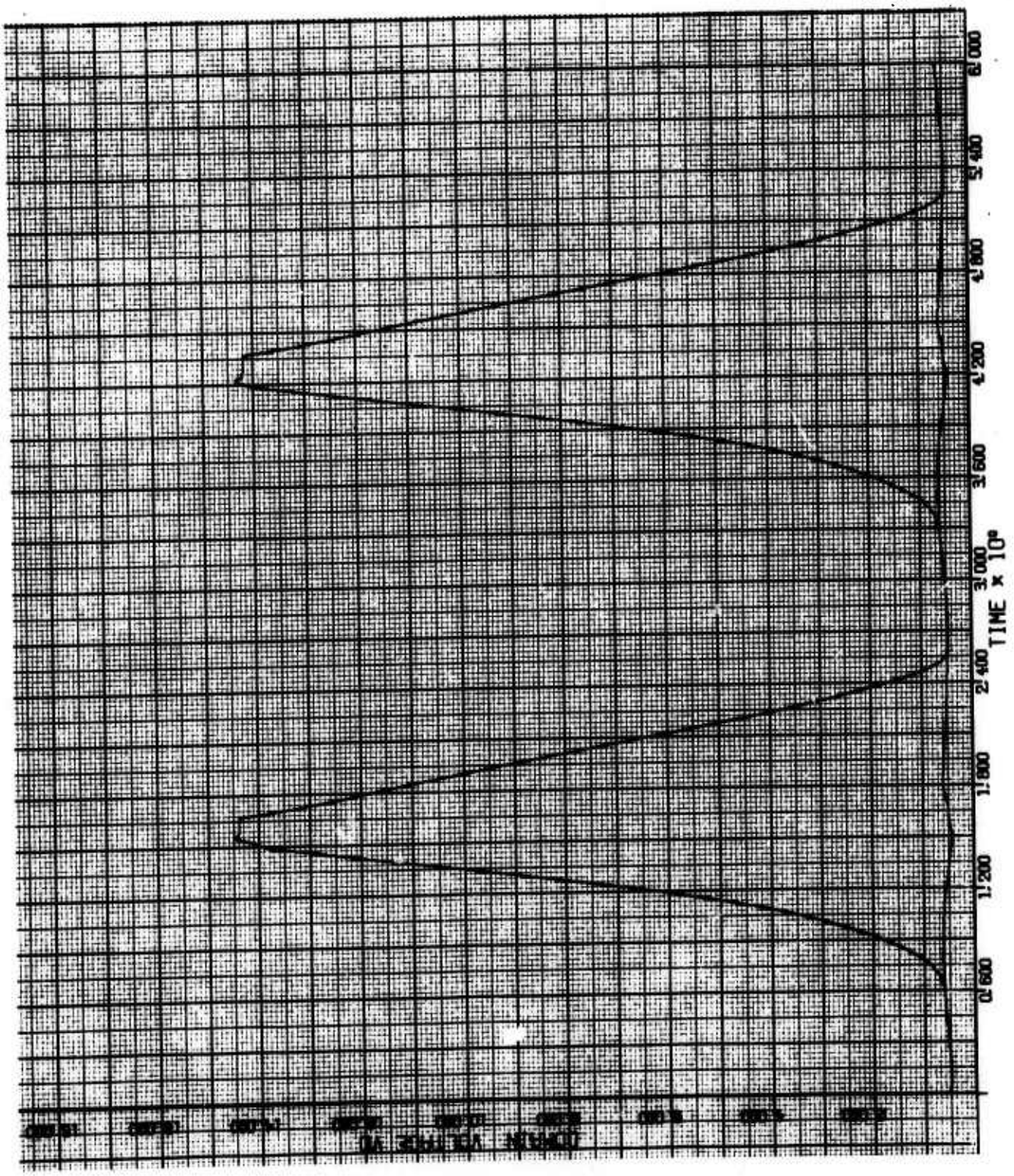

FIGURE 34: Domain Voltage for 1 Ohm and 2.5 nh Load

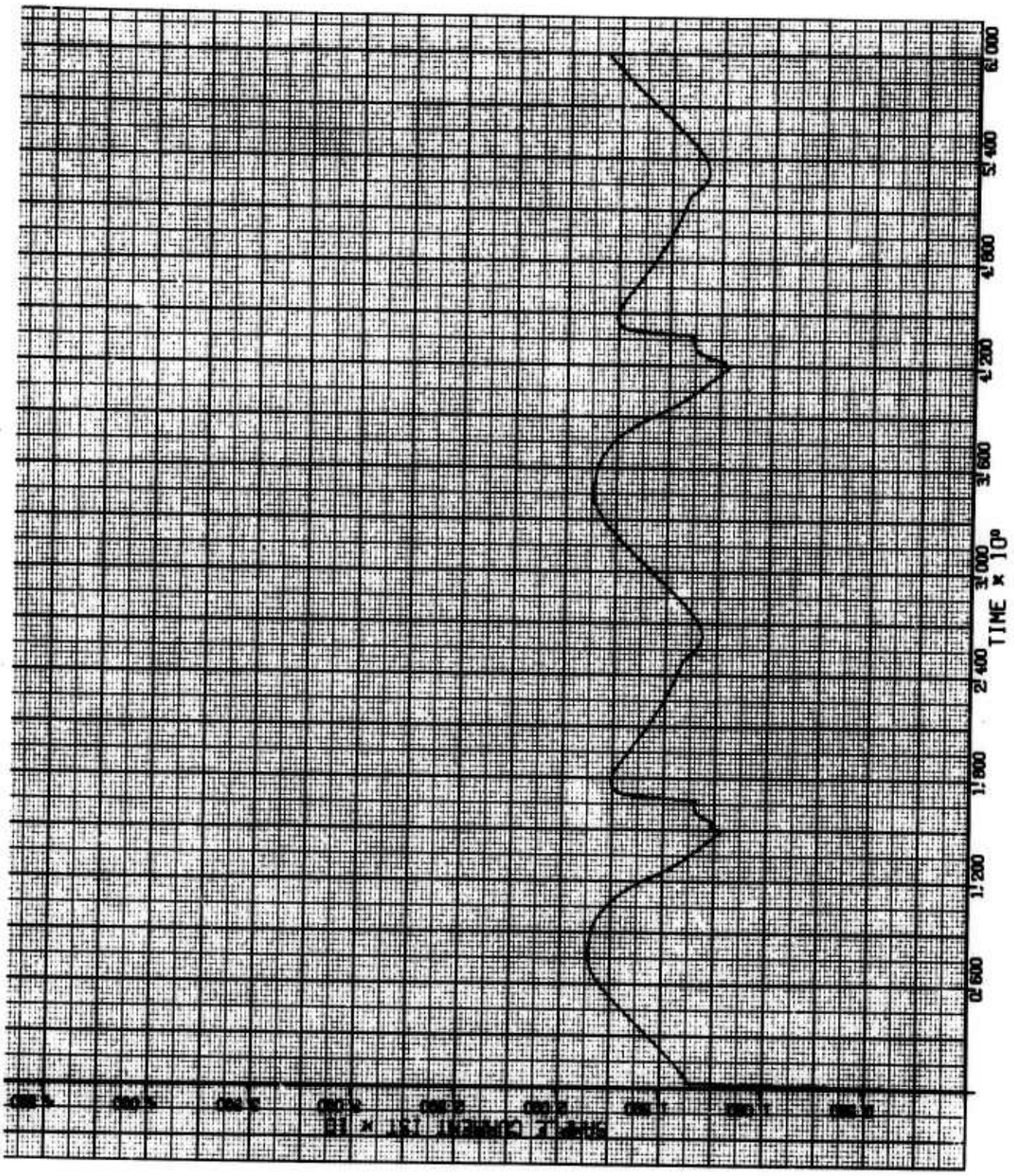

FIGURE 36: Device Current for 1 Ohm and 2.5 nh Load

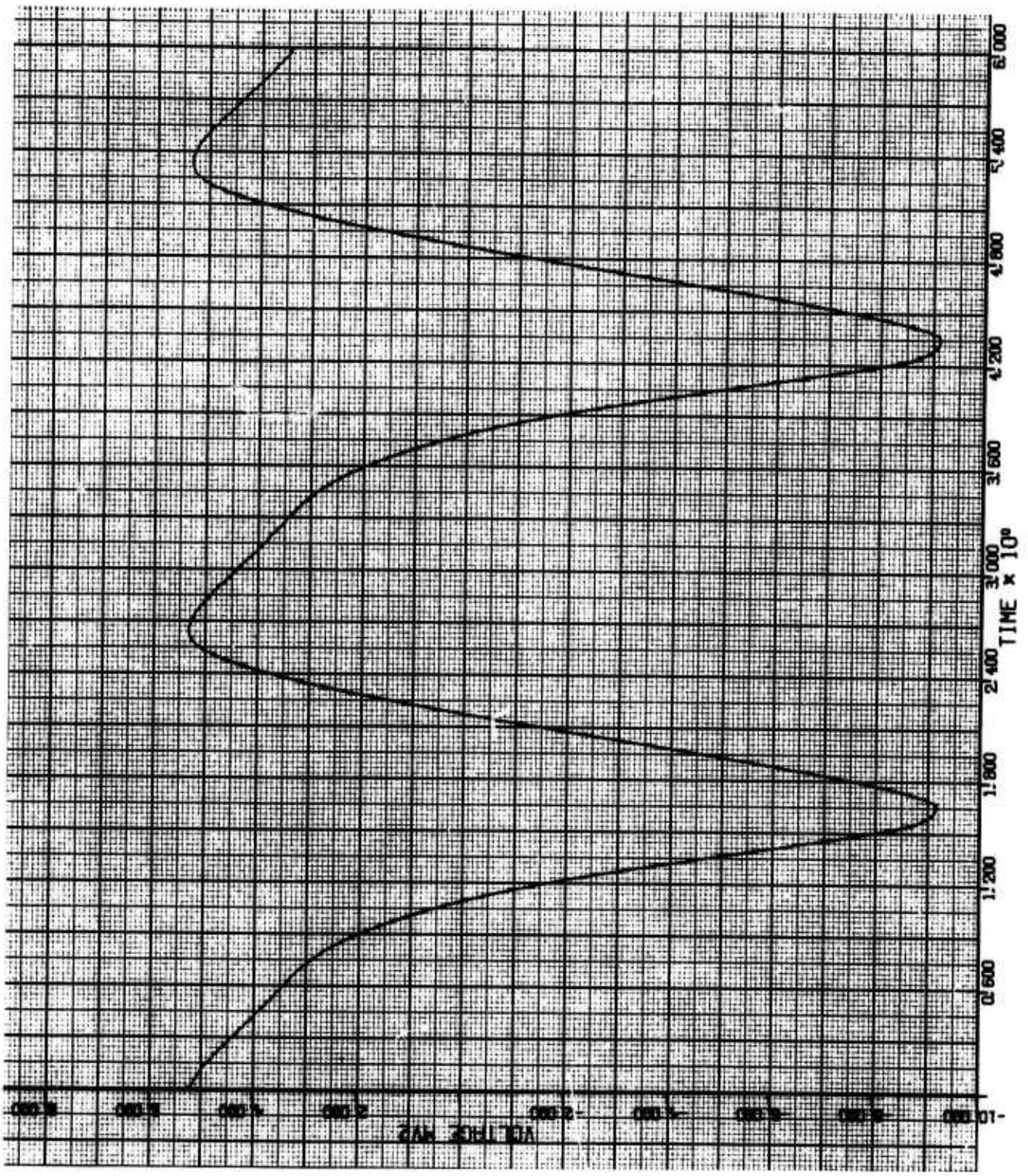

FIGURE 37: Inductor Voltage for 1 Ohm and 2.5 nh Load

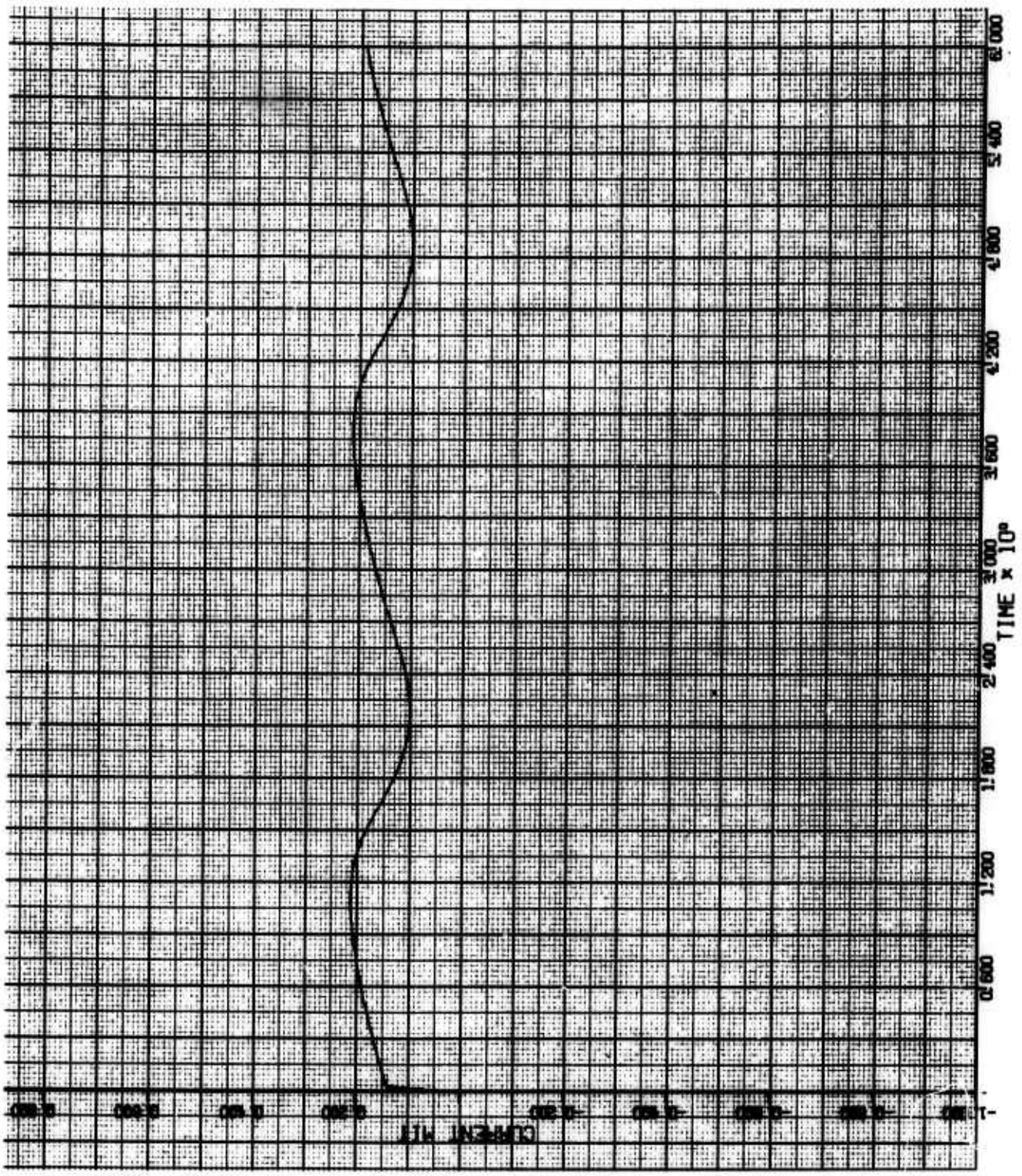

FIGURE 38: Microwave Circuit Current for 1 Ohm and 2.5 nh Load

as a function of time in Figs. 29 and 34, Figs. 30 and 35 and Figs. 32 and 37 respectively. The voltage of the bulk outside the domain, V_{RS}, and the bulk current I_{ST} are very closely in phase. This may be expected because of the small value of 0.05 pF for C_S.

A major difference between 0.5 nH and 2.5 nH calculations becomes obvious from the domain voltage plots in Figs. 29 and 34. For the low inductance case, the number of domains passing through the devices in a computation time of 6×10^{-10} sec is the same as for the case with no inductance (Fig. 22). However, only two domains are allowed through the device for the larger value of 2.5 nH for the inductance. With a 0.5 nH inductor, as the first domain is leaving the device, the rising voltage above V_{th} helps a new domain to form and to rapidly build up to maturity. Thus a favorable phase relation exists between the device voltage and the domain voltage V_D so that the sequence of domain triggering remains the same as for the case without an inductor. The stray capacitance MC_S and the device-domain system across it appear in parallel with the series combination of 1 ohm and 0.5 nH inductor to form a parallel resonant circuit. The domain, device and inductor voltages are nearly sinusoidal as are the device current I_{ST} and the inductor current MIT. I_{ST} and V_{ST} are very nearly 90° out of phase with I_{ST} leading V_{ST}. Therefore the bulk-domain system presents a capacitance at the sample contacts. The resonant frequency of M_{CS} and 0.5 nH is approximately 13.44 GHz and the operating frequency as determined from the repetition period of V_{ST} is 6.07 GHz. The difference between these two

frequencies can be accounted by an active-device capacitance of 1.1 pf, which is more than 20 times the electrostatic capacitance of the sample between contacts.

The different results obtained with 2.5 nH can be explained from the plots of domain and sample voltages shown in Figs. 34 and 35. It can be seen that as the first domain is disappearing, V_{ST} is below V_{th} and is decreasing so that a new domain is not actually allowed to form in the regular sequence as in the resistive case. The new domain does not begin to form until V_{ST} swings and stays above V_{th}. Thus, the phase relation between V_D and V_{ST} is made unfavorable by the 2.5 nH inductor for the domain-triggering sequence. The resonant frequency of 2.5 nH in parallel with M_{CS} is about 6.03 GHz. The operating frequency estimated from the period of V_{ST} is 3.71 GHz and once again, the difference in frequency can be accounted by a large active-device capacitance of 0.46 pF. Large active-device capacitances of this magnitude have actually been measured both in this Laboratory and by others. A concise explanation for this phenomenon is not known at present but it is suspected that the average negative resistance of the domain across its large capacitance connected in series with the low-field resistance of the bulk outside the domain may present a parallel combination of negative resistance and a large capacitance at the sample contacts. It should be mentioned, however, that the negative resistance and the capacitance of the active device will strongly depend on the bias voltage and on the external circuit connected to the device.

It may also be noted from Fig. 27 that the current MIT flowing

through the 1 ohm resistor connected in series with the 0.5 nH inductor is very nearly sinusoidal as opposed to the periodic pulses shown in Fig. 24 for the pure resistive load of 1 ohm. This can explain why the experimentally measured harmonics were more than 30 db down from the fundamental in one of the resistive test fixtures. This fixture had an effective inductance of the order of 0.5 nh. Small package and lead inductances can add up to a fraction of a nanohenry and consequently many of the harmonics of the device-current fundamental frequency will not appear across the 1 ohm load as in Fig. 33.

The facility with which the nonlinear, time-varying device interactions with microwave circuits can be handled by the computer model of the active Gunn device is clearly demonstrated. Calculations with this model show good agreement with some fundamental experiments. The interactions of cavity and other useful microwave circuits with the device will be studied in detail for possible improvement of device performance. Refinement of the model and additional applications will be investigated as a continuation of this work.

III. CONCLUSIONS

The noise performance of the recent solution-grown GaAs Gunn devices has been improved somewhat over the previous boat-grown material. As yet, no attempt has been made to provide a more optimum circuit configuration to minimize the noise, and the present noise performance should not be considered as the best available performance. The recent changes in the character of the noise have led to the possibility of identifying the source of noise in the device.

A circuit model has been implemented that retains both the time-dependent and non-linear device properties. The experimental correlations with this model have been encouraging to date, but the capabilities and limitations of the program are not fully known as yet.

REFERENCES

1. J. B. Gunn, IBM J. Res. Devl. 8, 141 (1964)

2. J. B. Gunn, Plasma Effects in Solids, 7th. Int. Conf. on the Physics of Semiconductors, Paris, 1964 (Academic Press Inc., New York, 1965) p. 199

3. J. S. Heeks, Trans. IEEE, Electron Devices, 13 , 68 (1966)

4. D. E. McCumber and A. G. Chynoweth, Trans. IEEE, Electron Devices, 13, 4 (1966)

5. J. A. Copeland, Trans. IEEE, Electron Devices, 13, 189 (1966)

UNCLASSIFIED

Security Classification

DOCUMENT CONTROL DATA - R&D

(Security classification of title, body of abstract and indexing annotation must be entered when the overall report is classified)

1. ORIGINATING ACTIVITY (Corporate author) Hewlett-Packard Company 1501 Page Mill Road Palo Alto, California 94304	2a. REPORT SECURITY CLASSIFICATION UNCLASSIFIED 2b. GROUP

3. REPORT TITLE

GUNN EFFECT DEVICES

4. DESCRIPTIVE NOTES (Type of report and inclusive dates)

Fourth Quarterly Technical Report - 15 August 1966 to November 1966

5. AUTHOR(S) (Last name, first name, initial)

M. L. Wright

6. REPORT DATE	7a. TOTAL NO. OF PAGES	7b. NO. OF REFS
February 1967	60	5

8a. CONTRACT OR GRANT NO.	9a. ORIGINATOR'S REPORT NUMBER(S)
DA 28-043 AMC-01758(E) b. PROJECT NO. ARPA Order No. 692 c. O/S Task No. 7900.21.243.38.00 d.	N/A 9b. OTHER REPORT NO(S) (Any other numbers that may be assigned this report) ECOM-01758-4

10. AVAILABILITY/LIMITATION NOTICES This document is subject to special export controls and each transmittal to foreign governments or foreign nations may be made only with prior approval of Commanding General, U. S. Army Electronics Command, Fort Monmouth, New Jersey, AMSEL-KL-SM.

11. SUPPLEMENTARY NOTES	12. SPONSORING MILITARY ACTIVITY
N/A	U. S. Army Electronics Command Fort Monmouth, New Jersey 07703 (AMSEL-KL-SM)

13. ABSTRACT

A third series of devices (PUAS) using commercially available boat-grown material has been fabricated and tested. This series is slightly thinner than the previous runs and shows a slightly lower threshold and a slightly higher Gunn frequency; in all respects they are quite similar to the previous results. The estimated contact resistance for the PUAS devices is about 8% of the bulk resistance.

Gunn effect devices have also been made from solution-grown GaAs material produced by Hewlett-Packard Laboratories. These devices show a positive temperature coefficient and thus require less power to operate. The noise level produced by these devices is lower than for the devices using boat-grown material especially at higher frequencies (~ 100Kc).

A circuit simulation for the Gunn device has been programmed for computer device-circuit interaction studies. This circuit model retains both the nonlinear and time-dependent characteristics of the device and has shown good correlation with several experimental results.

DD FORM 1 JAN 64 1473

UNCLASSIFIED

Security Classification

UNCLASSIFIED

Security Classification

14. KEY WORDS	LINK A		LINK B		LINK C	
	ROLE	WT	ROLE	WT	ROLE	WT
Microwave Oscillation Gunn Effect Devices						

INSTRUCTIONS

1. ORIGINATING ACTIVITY: Enter the name and address of the contractor, subcontractor, grantee, Department of Defense activity or other organization *(corporate author)* issuing the report.

2a. REPORT SECURITY CLASSIFICATION: Enter the overall security classification of the report. Indicate whether "Restricted Data" is included. Marking is to be in accordance with appropriate security regulations.

2b. GROUP: Automatic downgrading is specified in DoD Directive 5200.10 and Armed Forces Industrial Manual. Enter the group number. Also, when applicable, show that optional markings have been used for Group 3 and Group 4 as authorized.

3. REPORT TITLE: Enter the complete report title in all capital letters. Titles in all cases should be unclassified. If a meaningful title cannot be selected without classification, show title classification in all capitals in parenthesis immediately following the title.

4. DESCRIPTIVE NOTES: If appropriate, enter the type of report, e.g., interim, progress, summary, annual, or final. Give the inclusive dates when a specific reporting period is covered.

5. AUTHOR(S): Enter the name(s) of author(s) as shown on or in the report. Enter last name, first name, middle initial. If military, show rank and branch of service. The name of the principal author is an absolute minimum requirement.

6. REPORT DATE: Enter the date of the report as day, month, year, or month, year. If more than one date appears on the report, use date of publication.

7a. TOTAL NUMBER OF PAGES: The total page count should follow normal pagination procedures, i.e., enter the number of pages containing information.

7b. NUMBER OF REFERENCES: Enter the total number of references cited in the report.

8a. CONTRACT OR GRANT NUMBER: If appropriate, enter the applicable number of the contract or grant under which the report was written.

8b, 8c, & 8d. PROJECT NUMBER: Enter the appropriate military department identification, such as project number, subproject number, system numbers, task number, etc.

9a. ORIGINATOR'S REPORT NUMBER(S): Enter the official report number by which the document will be identified and controlled by the originating activity. This number must be unique to this report.

9b. OTHER REPORT NUMBER(S): If the report has been assigned any other report numbers *(either by the originator or by the sponsor)*, also enter this number(s).

10. AVAILABILITY/LIMITATION NOTICES: Enter any limitations on further dissemination of the report, other than those imposed by security classification, using standard statements such as:

(1) "Qualified requesters may obtain copies of this report from DDC."

(2) "Foreign announcement and dissemination of this report by DDC is not authorized."

(3) "U. S. Government agencies may obtain copies of this report directly from DDC. Other qualified DDC users shall request through _____."

(4) "U. S. military agencies may obtain copies of this report directly from DDC. Other qualified users shall request through _____."

(5) "All distribution of this report is controlled. Qualified DDC users shall request through _____."

If the report has been furnished to the Office of Technical Services, Department of Commerce, for sale to the public, indicate this fact and enter the price, if known.

11. SUPPLEMENTARY NOTES: Use for additional explanatory notes.

12. SPONSORING MILITARY ACTIVITY: Enter the name of the departmental project office or laboratory sponsoring *(paying for)* the research and development. Include address.

13. ABSTRACT: Enter an abstract giving a brief and factual summary of the document indicative of the report, even though it may also appear elsewhere in the body of the technical report. If additional space is required, a continuation sheet shall be attached.

It is highly desirable that the abstract of classified reports be unclassified. Each paragraph of the abstract shall end with an indication of the military security classification of the information in the paragraph, represented as *(TS)*, *(S)*, *(C)*, or *(U)*.

There is no limitation on the length of the abstract. However, the suggested length is from 150 to 225 words.

14. KEY WORDS: Key words are technically meaningful terms or short phrases that characterize a report and may be used as index entries for cataloging the report. Key words must be selected so that no security classification is required. Identifiers, such as equipment model designation, trade name, military project code name, geographic location, may be used as key words but will be followed by an indication of technical context. The assignment of links, rules, and weights is optional.

UNCLASSIFIED

Security Classification